Icarus 224 (2013) 347–363

Contents lists available at SciVerse ScienceDirect

Icarus

journal homepage: www.elsevier.com/locate/icarus

# Impact-generated hydrothermal systems on Earth and Mars

Gordon R. Osinski [a,b,c,*], Livio L. Tornabene [a,b], Neil R. Banerjee [a,b], Charles S. Cockell [d], Roberta Flemming [a,b], Matthew R.M. Izawa [a,b], Jenine McCutcheon [b], John Parnell [e], Louisa J. Preston [a,b], Annemarie E. Pickersgill [a,b], Alexandra Pontefract [a,b], Haley M. Sapers [a,b], Gordon Southam [a,b]

[a] Centre for Planetary Science and Exploration, University of Western Ontario, London, ON, Canada N6A 5B7
[b] Dept. of Earth Sciences, University of Western Ontario, London, ON, Canada N6A 5B7
[c] Dept. of Physics and Astronomy, University of Western Ontario, London, ON, Canada N6A 5B7
[d] School of Physics and Astronomy, University of Edinburgh, Edinburgh EH9 3JZ, UK
[e] Dept. of Geology, University of Aberdeen, Aberdeen AB24 3UE, UK

ARTICLE INFO

*Article history:*
Available online 1 October 2012

*Keywords:*
Impact processes
Cratering
Mars
Astrobiology

ABSTRACT

It has long been suggested that hydrothermal systems might have provided habitats for the origin and evolution of early life on Earth, and possibly other planets such as Mars. In this contribution we show that most impact events that result in the formation of complex impact craters (i.e., >2–4 and >5–10 km diameter on Earth and Mars, respectively) are potentially capable of generating a hydrothermal system. Consideration of the impact cratering record on Earth suggests that the presence of an impact crater lake is critical for determining the longevity and size of the hydrothermal system. We show that there are six main locations within and around impact craters on Earth where impact-generated hydrothermal deposits can form: (1) crater-fill impact melt rocks and melt-bearing breccias; (2) interior of central uplifts; (3) outer margin of central uplifts; (4) impact ejecta deposits; (5) crater rim region; and (6) post-impact crater lake sediments. We suggest that these six locations are applicable to Mars as well. Evidence for impact-generated hydrothermal alteration ranges from discrete vugs and veins to pervasive alteration depending on the setting and nature of the system. A variety of hydrothermal minerals have been documented in terrestrial impact structures and these can be grouped into three broad categories: (1) hydrothermally-altered target-rock assemblages; (2) primary hydrothermal minerals precipitated from solutions; and (3) secondary assemblages formed by the alteration of primary hydrothermal minerals. Target lithology and the origin of the hydrothermal fluids strongly influences the hydrothermal mineral assemblages formed in these post-impact hydrothermal systems. There is a growing body of evidence for impact-generated hydrothermal activity on Mars; although further detailed studies using high-resolution imagery and multispectral information are required. Such studies have only been done in detail for a handful of martian craters. The best example so far is from Toro Crater (Marzo, G.A., Davila, A.F., Tornabene, L.L., Dohm, J.M., Fairèn, A.G., Gross, C., Kneissl, T., Bishop, J.L., Roush, T.L., Mckay, C.P. [2010]. Icarus 208, 667–683). We also present new evidence for impact-generated hydrothermal deposits within an unnamed ~32-km diameter crater ~350 km away from Toro and within the larger Holden Crater. Synthesizing observations of impact craters on Earth and Mars, we suggest that if there was life on Mars early in its history, then hydrothermal deposits associated with impact craters may provide the best, and most numerous, opportunities for finding preserved evidence for life on Mars. Moreover, hydrothermally altered and precipitated rocks can provide nutrients and habitats for life long after hydrothermal activity has ceased.


## 1. Introduction

Hydrothermal systems have long been proposed as prime locations where life may have originated on Earth and, by analogy, on other planets such as Mars (e.g., Farmer, 2000). Hydrothermal systems can develop anywhere in the Earth's crust where a fluid (typically water) coexists with a heat source (Pirajno, 1992), with endogenic magmatic heat sources being predominant on Earth today (Farmer, 2000). On Mars, the conditions for the development of such systems were likely to have been met in the large-scale tectono-magmatic complexes of Tharsis and Elysium, as well as other smaller volcanic provinces (Schulze-Makuch et al., 2007). Like the Earth and the Moon, Mars also experienced the intense period of impact cratering early in its history. As with the Earth, but in contrast to the Moon, current models and observations also predict that Mars had a substantial initial endowment of $H_2O$ in both solid

* Corresponding author at: Dept. Earth Sciences, 1151 Richmond St., University of Western Ontario, London, ON, Canada N6A 5B7.
*E-mail address:* gosinski@uwo.ca (G.R. Osinski).

0019-1035/$ - see front matter © 2012 Elsevier Inc. All rights reserved.
http://dx.doi.org/10.1016/j.icarus.2012.08.030

(ice) and liquid (water) forms (Carr, 1996, 2006). The ancient highlands of Mars currently hold the oldest record of impact cratering on the planet, dating back to the end of the Late Heavy Bombardment (e.g., Strom et al., 2005). The martian highlands record abundant evidence of 'fluvial' erosion, in the form of the numerous small valley networks (Carr, 2006). While the exact conditions presiding over the formation of the small valley networks remain enigmatic, a strong case can be made that on early Mars, liquid $H_2O$ (the most plausible fluid) was abundantly available at and/or near the martian surface. It follows that hydrothermal systems on Mars, including those generated by impacts, were likely common and widespread (Schulze-Makuch et al., 2007).

In this contribution, we present a review of the record of impact-generated hydrothermal systems on Earth. The heat sources, mineralogy, and duration of these systems are summarized. We show that hydrothermal deposits can be found in six distinct settings within and around impact structures on Earth and we predict that the same is the case for Mars. We discuss the potential for the development of hydrothermal systems within martian impact craters and provide new observations for their origin. The potential for a record of life being preserved within, or peripheral to, such systems based on the terrestrial record is discussed. We also present a case study to demonstrate how difficult it can be, even with the analytical capabilities of laboratories on Earth, to prove that features are the result of biological activity. When the available evidence is synthesized, we suggest that impact-generated hydrothermal systems and their associated deposits represent prime exploration targets in the search for evidence of life on Mars.

## 2. Impact-generated hydrothermal systems: The record in terrestrial impact structures

We have conducted a review of hydrothermal alteration in terrestrial impact structures (Table 1), which builds upon earlier works (Naumov, 2002). Evidence for impact-generated hydrothermal activity is recognized at over 70 of the ~180 craters on Earth, from the ~1.8 km diameter Lonar Lake structure, India (Hagerty and Newsom, 2003), to the ~250 km diameter Sudbury structure, Canada (Ames et al., 1998). It is notable that very few simple craters display evidence for hydrothermal alteration, which accounts for ~50 craters in the Earth impact record. Thus, a reasonable hypothesis is that any hypervelocity impact capable of forming a complex crater (>2–4 and >5–10 km diameter on Earth and Mars, respectively) can potentially generate a *hydrothermal system*. Some exceptions may occur in extremely dry, arid environments, which has implications for other planetary bodies. It should be noted, however, that very few impact craters on Earth have been studied in detail and fewer still that concentrate on hydrothermal alteration specifically. Further work on this topic is urged.

In this contribution we use a general definition for hydrothermal activity that refers to the movement of warm (~50 °C) to hot (>500 °C) fluids in the subsurface (Pirajno, 1992). As discussed below, the degree of hydrothermal alteration of impact craters on Earth varies considerably, from discrete cavity and fracture filling to pervasive alteration of entire sequences or rock. Whether all these occurrences require *circulation* of hydrothermal fluids remains to be determined as scenarios could be invoked whereby an impact event could essentially provide a heat pulse capable of heating up preexisting $H_2O$ in rocks away from the impact site.

### 2.1. Heat sources

Impact events generate shock pressures and temperatures that can heat and/or melt substantial volumes of target material. The interaction of these impact-melted or heated materials with $H_2O$ in the near surface of a planet is capable of generating and sustaining a hydrothermal system. There are three main potential sources of heat for creating impact-generated hydrothermal systems (Osinski et al., 2005): (a) impact melt rocks and impact melt-bearing breccias; (b) elevated geothermal gradients in central uplifts; (c) energy deposited in central uplifts due to the passage of the shock wave. The size of the contribution of the latter is not clear at present, although it is generally assumed to be minor relative to the other two heat sources. The relative importance of heat from impact melt-bearing impactites versus central uplifts appears to be governed by crater size. In small- to medium-size structures (i.e., simple craters and complex craters up to ~20–30 km in diameter) the temperature increase imparted into the target rocks due to impact will typically range up to a maximum of ~100–120 °C. In larger 100 km-size structures, this can reach >1000 °C. As a result, in medium-size structures (e.g., Haughton, Ries; Table 1), impact melt-bearing impactites are the dominant heat source. In slightly larger structures (e.g., Manson, Puchezh-Katunki; Table 1), the central uplift may play a more major role consistent with the concentration of the highest temperature alteration minerals in the deeper central peak lithologies (Naumov, 2002). Because the production of impact melt does not scale linearly with increasing crater size, hydrothermal systems within the largest structures (e.g., the 250-km diameter Sudbury structure), may be dominated by heat contributed by impact melt-bearing impactites. It is also important to note that impact melt can form a substantial component of impact ejecta deposits (Osinski et al., 2011), the thickness of which will also scale with increasing crater size. No large basin-forming impacts are preserved on Earth but we predict that large hydrothermal systems may have been generated within the ejecta deposits of large martian basins (e.g., Hellas, Isidis, Argyre, Chryse, etc.), provided sufficient water was available.

### 2.2. Distribution of hydrothermal deposits

The impact cratering record on Earth provides the only existing ground-truth data on the distribution of hydrothermal sites within and around impact structures. Below, we distinguish six main locations in an impact crater where impact-generated hydrothermal deposits can form (Figs. 1 and 2). Field observations indicate that formation of hydrothermal deposits in impact craters is highly correlated with heat sources and/or the geometry of the fracture networks created by the impact event.

#### 2.2.1. Crater-fill impact melt rocks and melt-bearing breccias

In craters where impact melt-bearing deposits are preserved and where impact-generated hydrothermal activity occurred, impact melt-bearing impactites within the crater interior represent a major heat source for hydrothermal activity (Table 1). Mineralization within such lithologies ranges from being discrete, restricted to cavity and fracture fillings (e.g., Haughton; Fig. 2a), to completely pervasive (e.g., Ries). Where restricted, mineralization occurs preferentially towards the base and edges of the crater-fill impactites (Osinski et al., 2005). At the Ries structure, the crater-fill suevites are pervasively altered with complete replacement of all primary impact-generated glasses (Osinski, 2005a); alteration phases are zoned and vary distinctly with depth. At the Sudbury impact structure, pervasive hydrothermal alteration of crater-fill impact breccias (Onaping Formation) resulted in a series of regionally extensive semi-conformable alteration zones, above which occur zinc–lead–copper economic ore deposits (Ames et al., 1998).

The pervasive nature of the alteration at Sudbury is likely due to a combination of size and paleogeographic setting. At ~250 km in diameter, its heat sources kept hydrothermal circulation going for ~1 Ma, but the impact occurred in a shallow continental sea environment, ensuring that a continual source of water was present

**Table 1**
List of impact structures on Earth that preserve evidence for impact-generated hydrothermal alteration.

| | | | | | Hydrothermal Alteration | | | | | | | |
|---|---|---|---|---|---|---|---|---|---|---|---|---|
| | | | | | Setting | | | | | Impactite type | | |
| Crater Name | Location | Latitude | Longitude | Diameter (km) | Central Uplift | Crater-Fill Impactites | Ejecta | Rim | Unk. | Lithic Breccias/ Target Rocks | Impact Melt-Bearing Breccias | Impact Melt Rocks |
| Lonar | India | 19.97 | 76.52 | 1.83 | - | X | - | - | - | Mont | - | - |
| Holleford | Ontario, Canada | 44.47 | -76.63 | 2.35 | - | - | - | - | X | Chl, Ill | - | - |
| West Hawk | Manitoba, Canada | 49.77 | -95.18 | 2.44 | - | X | - | - | - | Cc, Sm, Sulf, Ill, Corr, At | - | Ze |
| Roter Kamm | Namibia | -27.77 | 16.29 | 2.5 | - | - | X | - | - | Qtz, Sulf, Chl, Ill | Cc | - |
| Rotmistrovka | Ukraine | 49.19 | 31.75 | 2.7 | - | - | - | - | X | Ze, Sm | - | - |
| Zapadnaya | Ukraine | 49.73 | 29.00 | 3.2 | - | - | - | - | X | Cc, Sm, Ill, Qtz, Ze, Chl, Sulf | Sm, Ze, Sd, Br, Kfsp, Sulf | Ze, Anh, Sulf |
| New Quebec | Quebec, Canada | 61.28 | -73.67 | 3.44 | - | X | X | | | Ep, Hem | - | - |
| Brent | Ontario, Canada | 46.08 | -78.48 | 3.8 | - | X | - | - | - | Chl, Hem, Cc, Prh | Ze, Cc, Sulf, Chl, Br | Chl, Sm, Qtz, Hem, Ze, Act |
| Flynn Creek | Tennessee, U.S.A. | 36.28 | -85.67 | 3.8 | X | | - | - | - | Cc | - | - |
| Kärdla | Estonia | 58.98 | 22.77 | 4 | X | X | - | - | - | Chl, Corr, Hem, Sulf, Ill | - | - |
| Mishina Gora | Russia | 58.72 | 28.05 | 4 | - | - | - | - | X | Chl, Cc, Kaol | - | - |
| Gardnos | Norway | 60.67 | 9.00 | 5 | - | X | - | - | - | - | Chl, Stp | - |
| Gow | Saskatchewan, Canada | 56.45 | -104.48 | 5 | - | X | - | - | - | Chl, Hem | Chl, Hem | Chl, Hem |
| Mizarai | Lithuania | 54.02 | 23.90 | 5 | - | - | - | - | X | Chl, Ep, Ze | - | Sm, Cc, Qtz, Chl, Ze |
| Söderfjärden | Finland | 63.03 | 21.58 | 5.5 | - | - | - | - | X | Cc, Chl, Ze | Ze | Chl, Ze |
| Jebel Waqf as Suwwan | Jordan | 31.05 | 36.81 | 5.5 | X | - | - | - | - | Cc, Ba | - | - |
| Decaturville | Missouri, U.S.A. | 37.90 | -92.72 | 6 | - | X | | | | Sulf | - | - |
| Pilot | Northwest Territories, Canada | 60.28 | -111.02 | 6 | - | - | - | - | X | Chl, Hem, Ser | - | - |
| Sääksjärvi | Finland | 61.42 | 22.38 | 6 | - | - | - | - | X | Ze, Chl, Qtz, Chc | - | Chl |
| Crooked Creek | Missouri, U.S.A. | 37.83 | -91.38 | 7 | X | X | - | - | - | Sulf, Qtz, Br | - | - |
| Lockne | Sweden | 63.00 | 14.82 | 7.5 | - | X | - | - | - | Cc, Sulf, Ze, Qtz | - | - |
| Wanapitei | Ontario, Canada | 46.75 | -80.75 | 7.5 | - | X | - | - | - | - | Sm, Ze | Op, Sm, Ze |
| Beyenchime-Salaatin | Russia | 71.06 | 121.69 | 8 | - | - | - | - | X | Sulf, Qtz | - | - |
| Couture | Quebec, Canada | 60.13 | -75.33 | 8 | - | - | - | - | X | Ep, Chl, Ser, Hem | - | - |
| Serpent Mound | Ohio, U.S.A. | 39.04 | -83.42 | 8 | X | - | - | - | - | Sulf | - | - |
| Ilyinets | Ukraine | 49.12 | 29.10 | 8.5 | - | - | - | - | X | Chl, Sm, Cc, Ze, Ab, Fu, Sulf | Sm, Ze, Qtz, Hem, Chl, Kfsp | Ze, Sm, Chl, Sulf, Cc, Fu, Br |
| Mien | Sweden | 56.42 | 14.87 | 9 | - | X | - | - | - | Chl, Ep, Ser | - | Sm, Ze, Qtz |
| Bosumtwi | Ghana | 6.50 | -1.42 | 10.5 | - | X | X | - | - | Chl, Ms, Ill | Chl, Ms | - |
| Ternovka (Terny) | Ukraine | 48.13 | 33.52 | 11 | - | - | - | - | X | Sm, Anh, Sulf, Br, Pb | - | Corr, Chc, Sulf, Cc, Stp, Op |
| Wells Creek | Tennessee, U.S.A. | 36.38 | -87.67 | 12 | X | X | - | - | - | Sm, Cc, Dl, Qtz, Sulf | - | - |
| Nicholson | Northwest Territories, Canada | 62.67 | -102.68 | 12.5 | - | X | - | - | - | Ep, Hem | - | - |
| Deep Bay | Saskatchewan, Canada | 56.41 | -102.99 | 13 | - | X | - | - | - | | Chl | - |
| Kentland | Indiana, U.S.A. | 40.75 | -87.40 | 13 | X | - | - | - | - | Cc, Py | - | - |
| Sierra Madera | Texas, U.S.A. | 30.60 | -102.92 | 13 | X | - | - | - | - | Cc, Py | - | - |
| Jänisjärvi | Russia | 61.97 | 30.96 | 14 | - | - | - | - | X | - | Chl, Cc, Ze | Qtz, Cc, Chl, Ep |
| Zhamanshin | Kazakhstan | 48.40 | 60.97 | 14 | - | - | - | - | X | - | Sm, Chl, Cc | - |
| Kaluga | Russia | 54.98 | 36.77 | 15 | - | - | - | - | X | Cc, Chl, Lm | Chl, Ze, Chc, Act | - |
| Logoisk | Belarus | 54.20 | 27.80 | 15 | - | - | - | - | X | Ze | Ab, Qtz, Chl | Chl, Ill |
| Ames | Oklahoma, U.S.A. | 36.25 | -98.20 | 16 | - | X | - | - | - | - | Cc | Cc, Qtz, Sm |
| Suavjärvi | Russia | 63.14 | 33.37 | 16 | - | | - | - | X | Sulf | - | - |
| El'gygytgyn | Russia | 67.50 | 172.08 | 18 | - | X | - | - | - | Qtz, Ze | - | - |

(*continued on next page*)

**Table 1** (*continued*)

| | | | | | Hydrothermal Alteration | | | | | | | |
|---|---|---|---|---|---|---|---|---|---|---|---|---|
| | | | | | Setting | | | | | Impactite type | | |
| Crater Name | Location | Latitude | Longitude | Diameter (km) | Central Uplift | Crater-Fill Impactites | Ejecta | Rim | Unk. | Lithic Breccias/ Target Rocks | Impact Melt-Bearing Breccias | Impact Melt Rocks |
| Dellen | Sweden | 61.83 | 16.75 | 19 | - | X | - | - | - | Sm | - | - |
| Obolon | Ukraine | 49.58 | 32.93 | 20 | - | | - | - | X | Cc, Sd | Sm, Chl | - |
| Gosses Bluff | Northern Territory, Australia | -23.82 | 132.31 | 22 | - | X | - | - | | Ze, Kfsp | - | - |
| Lappajärvi | Finland | 63.17 | 23.67 | 23 | - | | - | - | X | Ze | Ze, Sm, Cc | Sm, Chl, Cc, Chc, Hem |
| Rochechouart | France | 45.83 | 0.93 | 23 | - | X | - | - | - | Chl, Corr, Cc, Sulf | Chl, Sm, Sulf | Chl, Qtz |
| Haughton | Nunavut, Canada | 75.37 | -89.68 | 23 | X | X | X | X | - | Cc, Qtz, Py, Marc | - | Cc, Marc, Fl, Ba, Py |
| Boltysh | Ukraine | 48.95 | 32.29 | 24 | X | X | - | - | - | Sm, Chl, Ep, Ze, Cc, Grt | - | Sm, Chl, Cc, Ze, Stp, Sulf |
| Ries | Germany | 48.88 | 10.62 | 24 | - | X | X | X | - | Sm, Cc, Chl, Ze, Anh, Corr, Qtz | Sm, Ze, Ill | - |
| Kamensk | Russia | 48.37 | 40.49 | 25 | - | - | - | - | X | Cc, Sulf | Cc, Sm, Chl, Ze | - |
| Steen River | Alberta, Canada | 59.50 | -117.63 | 25 | - | X | - | - | - | Ze, Qtz, Chl, Ca | Sm, Ze | - |
| Strangways | Northern Territory, Australia | -15.20 | 133.59 | 25 | - | X | - | - | - | - | Sm | - |
| Clearwater East | Quebec, Canada | 56.50 | -74.70 | 26 | - | X | - | - | X | Sm, Chl, Cc, Hem | - | Sm, Qtz, Cc, Sulf, Hem |
| Mistastin | Newfoundland/ Labrador, Canada | 55.53 | -63.18 | 28 | - | X | X | - | - | Chl, Ser, Ze | - | Sm, Cc, Qtz, Chl, Ze |
| Slate Islands | Ontario, Canada | 48.40 | -87.00 | 30 | X | - | - | - | - | Hem, Chl | Sm, Chl | - |
| Shoemaker | Western Australia, Australia | -25.87 | 120.88 | 30 | X | - | - | - | - | Qtz, Ab, Kfsp, Cpx, Preh, Sm | - | - |
| Yarrabubba | Western Australia, Australia | -27.17 | 118.83 | 30 | X | - | - | - | - | Cc, Qtz, Kfsp, Fl, Preh, Chl | - | - |
| Manson | Iowa, U.S.A. | 42.35 | -94.33 | 35 | X | X | - | - | - | Chl, Corr, Qtz, Sm, Ill, Grt, Act, Prh, Ep | Sm, Corr, Chl, Ze, Qtz, Sulf | - |
| Clearwater West | Quebec, Canada | 56.08 | -74.12 | 36 | - | X | - | - | - | | - | Sm, Hem |
| Carswell | Saskatchewan, Canada | 58.45 | -109.50 | 39 | - | - | - | | X | Chl, Ill, Sulf, Cc, Hem, Coff | Chl, Cc, Sulf, Pb | Chl, Qtz, Ze |
| Araguainha | Brazil | -16.81 | -52.99 | 40 | X | X | - | - | - | Qtz, Hem | - | Chl, Qtz, Cc, Fu |
| Woodleigh | Western Australia, Australia | -26.06 | 114.66 | 40 | X | - | - | - | - | Al, Qtz, Ill, Chl, Cc Marc, Py | - | - |
| Saint Martin | Manitoba, Canada | 51.78 | -98.53 | 40 | X | X | - | - | X | Cc, Ze, Sm | Cc | Sm, Chl, Cc, Qtz |
| Siljan | Sweden | 61.03 | 14.87 | 52 | X | - | - | - | - | Sm, Chl, Ze, Ep, Ab, Sulf, Hem | - | - |
| Charlevoix | Quebec, Canada | 47.53 | -70.30 | 54 | X | X | - | - | - | Ze, Cc, Prh, Qtz | - | Chl, Sm, Qtz |
| Beaverhead | Montana, U.S.A. | 44.64 | -113.00 | 60 | - | - | - | - | X | Chl, Qtz, Corr, Cc, Kfsp, Sulf | - | - |
| Kara | Russia | 69.10 | 64.26 | 65 | - | X | - | - | - | Cc, Sulf, Ze, Apf, Br | Sm, Cc, Sulf, Ze, Op | Sm, Chl |
| Puchezh-Katunki | Russia | 56.97 | 43.72 | 80 | X | - | - | - | - | Sm, Ze, Chl, Anh, Cc, Sulf, Apf, Act, Grt, Ab, Gp, Qtz, Ep, Prh | Sm, Ze, Cc, Op | Sm, Ze, Cc |
| Chesapeake Bay | Virginia, U.S.A. | 37.25 | -76.02 | 90 | - | X | - | - | - | Sm, Chl, Ill, Mont, Cc, Qtz, Ze, Ab, Epid | Sm, Cc | - |
| Manicouagan | Quebec, Canada | 51.38 | -68.70 | 100 | X | X | - | - | - | Ze, Chl, Hem | - | Sm, Qtz, Chl, Ze, Hem |
| Popigai | Russia | 71.64 | 111.23 | 100 | ? | X | - | - | - | Sm, Cc, Anh, Chl, Ze, Prh, Grt, Gp | Sm, Cc, Chl, Sulf, Ze, Qtz, Gp, Ep, Op | Sm, Chl, Qtz, Ze, Ill, Cc, Sulf, Op, Act |
| Chicxulub | Yucatan, Mexico | 21.30 | -89.50 | 170 | X | X | X | - | - | Kfsp, Mag, | Sm, Anh, Sulf, Chl, Kfsp, Py, Qtz, Alb, Mag, | Ep, Qtz, Ab, Kfsp, Cc, Sm, An, Cc, Mag, Chl |
| Sudbury | Ontario, Canada | 46.60 | -81.18 | 250 | X | X | X | - | - | - | Chl, Act, Sulf, Cc, Sm, Ep, Sph | - |

*Abbreviations*: Ab = albite; Act = actinolite; An = anatase; Anh = anhydrite; Ba = barite; Cc = calcite; Chc = chalcopyrite; Chl = chlorite; Cpx = clinipyroxene; Ep = epidote; Fl = fluorite; Hem = hematite; Kfsp = K-feldspar; Ill = illite; Mag = magnetite; Marc = marcasite; Mont = montmorillonite; Qtz = quartz; Prh = prehnite, Prh = pyrrhotite; Sm = smectite; Sulf = sulfur; Sph = sphalerite; Ze = zeolite.

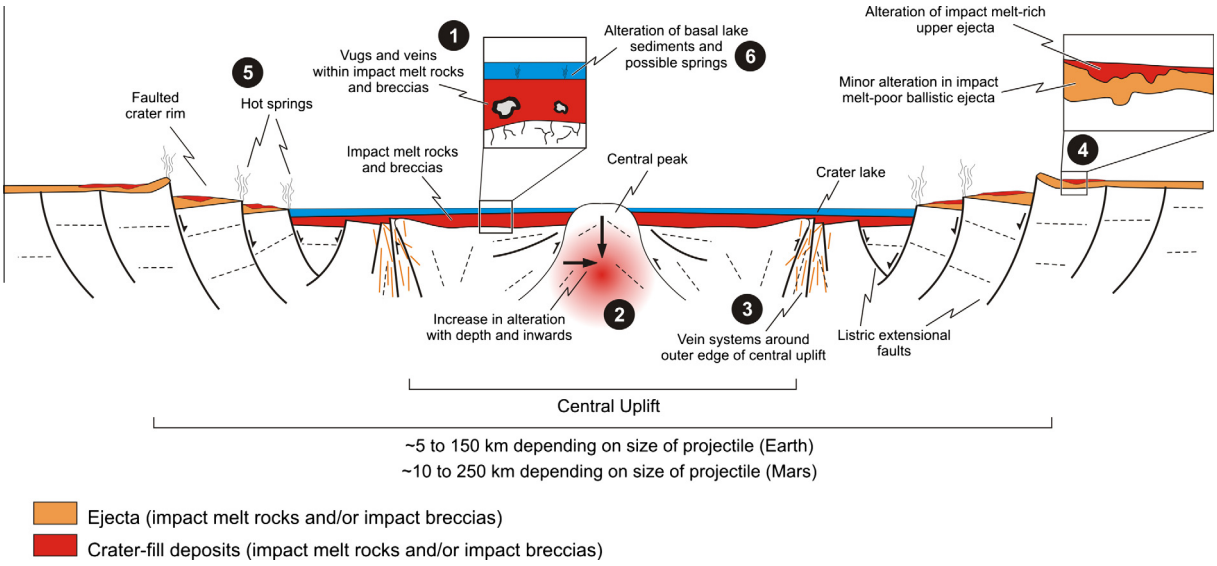


**Fig. 1.** Distribution of impact-generated hydrothermal alteration deposits within and around a typical complex impact crater. The six settings are highlighted and numbered in the order in which they are discussed in the text.

(Ames et al., 1998). This is consistent with differences between the level of alteration within the Kara, Popigai, and Puchezh-Katunki impact structures, Russia (Table 1), where the most intensive impact-generated hydrothermal alteration took place in the craters that formed in shallow continental shelf or intra-continental shallow basins (e.g., Kara and Puchezh-Katunki) (Naumov, 2002). The difference in the intensity of hydrothermal alteration of crater-fill impactites between the Haughton and Ries impact structures is notable given their similar size (23 and 24 km, respectively) and the fact that they both occurred in a continental setting. Critically, the crater-fill suevites at the Ries are overlain by ~400 m of lacustrine crater-fill sediments and sedimentation appears to have commenced immediately following impact (Arp, 1995). In contrast, at Haughton, there is no evidence preserved of a crater lake immediately post-impact (Osinski and Lee, 2005). This suggests that the presence/absence of an overlying crater lake may play a critical role in determining the level of hydrothermal alteration of crater-fill impactites.

### 2.2.2. Interior of central uplifts

In many terrestrial impact structures, erosion has removed the superficial crater-fill impactites. This is reflected in the large number of sites where hydrothermal alteration has only been documented in the more deep-seated lithologies of central uplifts (Table 1). As noted above, central uplifts are formed during the modification stage of complex impact crater formation and their uplifted geotherms can contribute a heat source driving hydrothermal systems. Central uplifts form in craters >2–4 km diameter on Earth, and >5–10 km on Mars (Melosh, 1989) and are comprised of fault-bounded blocks of coherent to brecciated bedrock commonly with injection dykes of impact melt-bearing or melt-free impact breccias. Mineralization within such lithologies is typically discrete and restricted to vug and vein filling cavities and along fractures (Fig. 2b). Deep drilling of a number of structures, such as the ~35 km diameter Manson (McCarville and Crossey, 1996) and ~80 km diameter Puchezh-Katunki (Naumov, 2002) impact structures, reveal a zoned alteration assemblage with inferred hydrothermal mineral crystallization temperatures that increase both with depth and towards the crater center (Fig. 1).

### 2.2.3. Outer margin of central uplifts

Structural studies of complex impact structures have shown that the outer margins of central uplifts are often highly fractured and faulted because they represent an interference zone where the inwards-collapsing crater walls interact with the outwards-collapsing edge of the central uplift (Kenkmann and von Dalwigk, 2000; Osinski and Spray, 2005). Not surprisingly, these zones commonly represent sites of more intense hydrothermal alteration, particularly the infilling of fractures to form vein networks (Figs. 1 and 2c) (Hode et al., 2003; Osinski et al., 2005). Observations from Haughton suggest that these outer central uplift regions are buried under crater-fill impact melt rocks and breccias in fresh craters.

### 2.2.4. Ejecta deposits

Impact ejecta deposits are characteristic features of fresh impact craters on Earth and other planets. Such deposits are superficial in nature, typically tens of meters thick for craters <100 km in diameter and as a result of erosion are rarely preserved on Earth. An important observation is that ejecta deposits appear to be comprised of (at least) two distinct facies or layers in many craters on the terrestrial planets (Osinski et al., 2011). The Ries structure in Germany is an excellent example, where a patchy layer of impact melt-bearing breccia overlies melt-free lithic breccias (Bunte Breccia). Importantly, the Bunte Breccia deposits were emplaced at ambient temperatures and no evidence of hydrothermal alteration has been documented (Hörz, 1982). The overlying impact melt-bearing breccias, in contrast, were emplaced at temperatures >750–900 °C (Osinski et al., 2004).

A range of "secondary" minerals have been documented within the impact melt-bearing breccias, with montmorillonite clay and zeolite minerals being the dominant assemblages (Fig. 2d). Complications with the origin of these assemblages arise due to the nature of the groundmass. In particular, there is evidence for two generations of hydrous silicates with an early undetermined groundmass-forming phase, potentially formed through devitrification or autometamorphism of hydrous impact glasses (Osinski et al., 2004), and later cross-cutting veins of platy montmorillonite clay (Osinski, 2005a). Some favor a hydrothermal origin for at least some of these clays (Newsom et al., 1986; Osinski, 2005a), while others, based on stable isotope studies, suggest a low-temperature origin (<20 °C) (Muttik et al., 2010). However, these lower temperatures are based on studies of bulk samples so that it is unclear what generation of hydrous silicates were analyzed and/or whether this represents a modern-day overprint of an originally higher temperature assemblage. Regardless of these complications, it appears that the

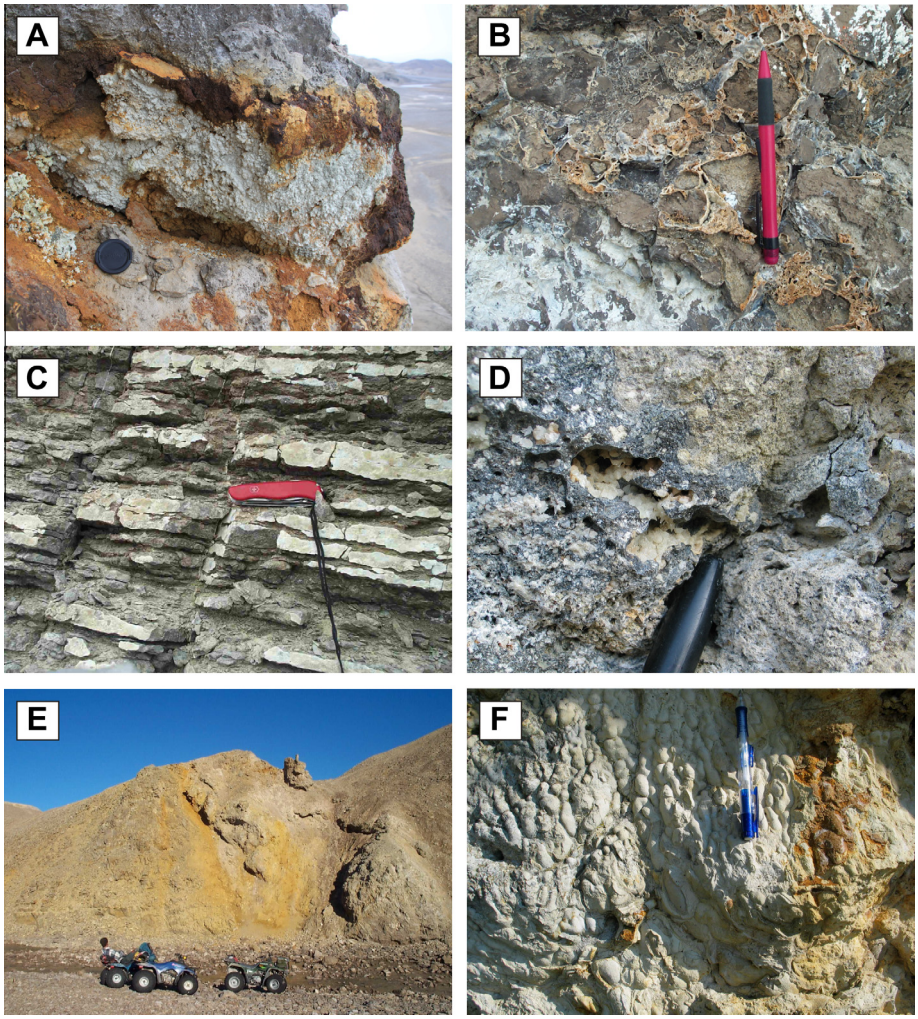


**Fig. 2.** Field photographs showing the six different types of hydrothermal alteration shown schematically in Fig. 1. (a) Mineralization within crater-fill impact melt rocks at the Haughton impact structure, Canada. The vug is dominated by marcasite (rusty green) and calcite mineralization. Pale green accumulations of fibroferrite with copiapite, gypsum, and rozenite in the center of the image: 7 cm diameter lens cap for scale. (b) Brecciated rocks of the central uplift of the Haughton structure cemented by hydrothermal quartz: 14 cm long pencil for scale. (c) Pervasive calcite veining around the edge of the central uplift at the Haughton structure: 10 cm long penknife for scale. (d) Alteration of ejecta deposits at the Ries impact structure, Germany. Cavities within impact glasses in impact-melt bearing breccias are lined by sparry calcite. The tip of a marker is at the bottom of the image and is 1 cm across. (e) Hydrothermal pipe structures interpreted as paleo-hydrothermal vents around the faulted crater rim region of the Haughton structure. Two structures are shown in this image highlighted by intense goethite alteration (orange). Person and All-Terrain Vehicles for scale. (f) Stromatolite-bearing intra-crater lacustrine sediments within the Ries structure: 13 cm long pencil for scale. (For interpretation of the references to color in this figure legend, the reader is referred to the web version of this article.)

intensity of hydrothermal alteration of the Ries impact melt-bearing breccias does vary considerably and some outcrops are intensely altered. These deposits are always overlain, or were overlain, by sedimentary crater-fill deposits such that the presence/absence of an overlying crater lake played a critical role in determining the level of hydrothermal alteration of impactites at the Ries impact structure (cf., crater-fill impactites, see Section 2.2.1).

It is also important to note that the heat source for the alteration of ejecta deposits comes entirely from the deposits themselves. In particular, impact melt volumes increase with increasing crater size (Grieve and Cintala, 1992). Therefore, crater size strongly affects the longevity of the heat source, and hence the pervasiveness of hydrothermal alteration. These observations are particularly important with respect to Mars, where the focus of impact-generated hydrothermal models has exclusively focused on crater interiors (e.g., Rathbun and Squyres, 2002; Abramov and Kring, 2005; Schwenzer and Kring, 2009). Because of this, alteration phases within the ejecta deposits have tended to be interpreted as excavated preexisting target material (e.g., Ehlmann et al., 2011). Although impact excavation is viable for explaining alteration phases in crater ejecta, the observations at the Ries impact structure demonstrate that there are other possible explanations that include impact-generated alteration mechanisms.

### 2.2.5. Crater rim

The rims of complex impact craters are regions where large km-scale, typically listric, extensional faults are common. These faults and the surrounding fractured rocks provide excellent fluid pathways for hydrothermal fluids. Unfortunately, very few craters have adequate preservation and surface exposure in the rim region to assess this hypothesis. The one medium-sized complex impact structure where the rim has been mapped in detail and that presents excellent exposure is the Haughton structure in the Canadian Arctic (Osinski, 2005b). Detailed field mapping has revealed the presence of a complexly faulted rim region. The same mapping documented over seventy hydrothermal "pipe" structures (Fig. 1) (Osinski et al., 2001; Osinski et al., 2005). These sub-vertical cylindrical structures range from ~1 to ~5 m across and are exposed

over lengths of up to 20 m (Fig. 2e). They are characterized in the field by pronounced Fe-hydroxide alteration of the country rocks. They are developed exclusively around the rim where faulting occurs and have not been documented in the impact melt rocks in the crater's central area or in the central uplift (Osinski et al., 2001; Osinski et al., 2005). Importantly, these pipe structures have been interpreted as hydrothermal vents, whose surficial expressions were likely hot springs and/or fumaroles (Osinski et al., 2005).

#### 2.2.6. Post-impact crater lake sediments

Impact craters can provide protected sedimentary basins that can provide hospitable environments for sustaining communities of primitive microorganisms and may increase the preservation potential of fossils and organic material (Figs. 1 and 2f). Furthermore, heat from an impact event is capable of generating a lake even in areas of permafrost (i.e., permanently frozen ground). Intra-crater sedimentary deposits may, therefore, hold valuable clues to the pace of recovery of the environment and post-impact biological succession following large impact events (Cockell and Lee, 2002). Given the theorized requirement of liquid $H_2O$ for life, impact crater lake deposits have long been suggested as important targets in the search for evidence of past life on Mars (Cabrol et al., 1999), which is one of the reasons why the Mars Science Laboratory mission, Curiosity, will investigate the post-impact sedimentary deposits within the 155 km diameter Gale crater.

Impact crater lakes are common in terrestrial craters but they, and their associated sediments, have received relatively little attention as most work has focused on the paleoclimate record retained in such deposits. Intriguingly, if a crater lake formed shortly after impact, it is likely that the basal sediments deposited within the lake would have been altered by the impact-generated hydrothermal system. Evidence for such alteration has been documented at the Boltysh and Ries structures, where a variety of clays and zeolites have been documented in the basal intra-crater lacustrine sediments (Salger, 1977; Jolley et al., 2010) (Fig. 2f). In contrast, other intra-crater sedimentary deposits, such as those at the Haughton impact structure, do not show signs of hydrothermal overprinting. The apparent lack of alteration in the Haughton lake sediments may be a result of deposition occurring >10 Ma after the impact event (Osinski and Lee, 2005). It has, however, been shown at Haughton, that organic geochemical signatures can be transferred from bedrock to these post-impact sediments, thus surviving the impact event (Parnell et al., 2008). It is, therefore, highly plausible that any organic geochemical signature will be transferred to crater lake sediments, whether that signature was formed pre- or syn-impact.

### 2.3. Duration

The duration of impact-generated hydrothermal systems represents one of the least well-understood aspects of the process. In general, the lifetime of an impact-generated hydrothermal system will increase with crater size as the size and longevity of the heat sources also increases. This increase does not, however, appear to be linear. At the 4-km diameter Kärdla crater, estimates suggest that cooling to temperatures below 90 °C took ~1500–4500 years (Jõeleht et al., 2005). This compares to ~1 myr for the hydrothermal system within the ~250-km diameter Sudbury impact structure (Ames et al., 1998). This is generally consistent with numerical modeling, which yielded estimates of 0.2–3.2 Ma for Sudbury (Abramov and Kring, 2004) and 1.5–2.3 Ma the 180-km diameter Chixculub impact structure (Abramov and Kring, 2007); the large uncertainties are due to large ranges of modeled permeabilities.

### 2.4. Mineralogy of hydrothermal deposits

We propose that impact-generated hydrothermal minerals can be grouped into three broad categories: (1) hydrothermally-altered target-rock assemblages; (2) primary hydrothermal minerals precipitated from solutions; and (3) secondary assemblages formed by the alteration of primary hydrothermal minerals. Target lithology strongly influences the hydrothermal mineral assemblages formed the post-impact hydrothermal systems. As noted in Section 2.3, the amount of energy deposited by the impact event influences the duration and intensity of hydrothermal activity, which in turn influences the alteration assemblages produced by the system. In general, larger, longer-lived post-impact hydrothermal systems create more extensive hydrothermal mineral deposits and cause more alteration of preexisting target rock assemblages (Table 1). The composition of fluids (i.e. meteoric water, sedimentary pore waters, brines, and seawater) also influences the final mineral assemblage. Post-impact hydrothermal mineralization processes are similar to those driven by endogenic heat sources, except that post-impact hydrothermal systems are always characterized by a retrograde sequence of alteration minerals due to progressive cooling (e.g., Naumov, 2005).

#### 2.4.1. Target rock alteration assemblages

Post-impact hydrothermal activity can produce numerous mineralogical changes in preexisting, potentially impact-modified, target rocks. Our review suggests that the alteration of silicates and impact melt (minerals and glasses) commonly leads to the production of hydrated silicate phases, such as phyllosilicates (Table 1) (including clay minerals, e.g., saponite, montmorillonite, celadonite, kaolinite, halloysite; also chlorite-group minerals, and micas). Chemical exchange between hydrothermal solutions and target rocks may cause a wide variety of mineralogical and mineral–chemical changes, particularly in the largest impact structures such as Chicxulub (Zürcher and Kring, 2004), Vredefort (Grieve and Therriault, 2004) and Sudbury (Ames et al., 2006). Mineral assemblages created by exchange with hydrothermal fluids overprint the existing target rock assemblage(s). It is common for multiple generations of hydrothermal minerals to be present, particularly in large structures (e.g., Ames et al., 2006; Zürcher and Kring, 2004). Observations of the overprinting relationships between minerals are invaluable for elucidating physicochemical evolution of post-impact hydrothermal systems.

#### 2.4.2. Primary hydrothermal mineral assemblages

Primary hydrothermal minerals are those minerals precipitated from hydrothermal solutions. Impact-generated hydrothermal systems, like all hydrothermal systems, may precipitate a vast number of new mineral phases depending on local physicochemical conditions. Table 1 provides a summary of important post-impact hydrothermal mineral occurrences. Below, we briefly review the major mineral groups documented in terrestrial impact-generated hydrothermal systems.

*2.4.2.1. Silicates.* Silica minerals and mineralloids including quartz, chalcedony, amorphous silica and opal are common post-impact hydrothermal minerals. Quartz is commonly associated with early, high-temperature stages of hydrothermal alteration (e.g., Ames et al., 2006; Osinski et al., 2005). Other silicates include hydrothermal K-feldspar (adularia), epidote, amphibole-group minerals (e.g., tremolite–actinolite), phyllosilicates, and zeolites. Silica minerals are important for the preservation of biological materials (e.g., Preston et al., 2008).

*2.4.2.2. Carbonates.* Carbonates are common constituents of post-impact hydrothermal deposits, with calcite and dolomite dominating (Table 1). Calcite may form spectacular 'flowstone' or "travertine" deposits, resembling those found at geothermal sites (e.g., Osinski et al., 2005), but is more typically found in veins and vugs. Carbonate mineralization is commonly a feature of distal, low-temperature areas of hydrothermal systems and late-stage hydrothermal activity.

*2.4.2.3. Sulfides.* The $FeS_2$ polymorphs marcasite and pyrite are very common post-impact hydrothermal minerals (Table 1). Others reported include bornite, chalcopyrite, sphalerite, galena, pyrrhotite, pentlandite, arsenopyrite, niccolite, covellite, and millerite. In large impact structures (e.g., Sudbury) sulfides (re-)precipitated in post-impact hydrothermal processes can be a significant economic resource (Grieve, 2005).

*2.4.2.4. Native elements and alloys.* Traces of native gold, electrum, silver, and platinum-group element (PGE) alloys are associated with hydrothermal sulfides in the Sudbury structure (Ames et al., 2008).

*2.4.2.5. Oxides and oxyhydroxides.* Primary hydrothermal magnetite, anatase, and ilmenite have been documented in the Yaxcopoil-1 core at the Chicxulub crater (Zürcher and Kring, 2004).

*2.4.2.6. Sulfates.* Gypsum is a common late hydrothermal product, particularly at the Haughton impact structure, and such deposits may reflect hydrothermal remobilization of sulfates in the target rocks. Barite and celestite have also been documented in post-impact hydrothermal deposits at Haughton (Osinski et al., 2005) and Chicxulub (Zürcher and Kring, 2004). Gypsum crystals can provide important habitats for microbial life in impact structure settings (Cockell et al., 2010).

*2.4.2.7. Halides.* Fluorite has been reported from the Haughton impact structure (Osinski et al., 2005). Halite is a common phase in hydrothermal fluid inclusions in post-impact hydrothermal settings. Recrystallized halite has been reported from marine impact settings such as Chicxulub (Zürcher and Kring, 2004).

*2.4.3. Secondary ("weathering") mineral assemblages*

Secondary post-impact hydrothermal mineral assemblages are those associated with the alteration, weathering, and/or remobilization of primary hydrothermal minerals. Because they would not exist if their precursor assemblages had not been produced by hydrothermal processes, we consider them part of the spectrum of post-impact hydrothermal minerals. Hydration and oxidation are both important processes in the formation of secondary assemblages, particularly Fe-sulfates and Fe-oxyhydroxides. Secondary mineral assemblages and processes are of potential significance for microbial colonization of the post-impact environment and the preservation of biological materials (Izawa et al., 2011). The only detailed study of such processes comes from the Haughton impact structure (Izawa et al., 2011) and the mineral assemblages are detailed below.

*2.4.3.1. Sulfates.* Numerous Fe-sulfates are produced during the weathering of primary Fe-sulfides, including melanterite, schwertmannite, rozenite, szomolnokite, jarosite, fibroferrite, and copiapite. Primary hydrothermal gypsum may be remobilized and reprecipitated as fine-grained crusts and coatings.

*2.4.3.2. Oxyhydroxides.* Ferrihydrite and goethite are both common alteration products of primary sulfides. Goethite in particular is a common end product of Fe-sulfide weathering, and may pseudomorphically replace primary sulfide crystals. Under very arid conditions, goethite may alter further to hematite.

## 3. The astrobiological significance of impact-generated hydrothermal systems

The motivation for this contribution derives from the long-standing suggestion that hydrothermal systems might have provided habitats or "cradles" for the origin and evolution of early life on Earth, and possibly other planets such as Mars (Farmer, 2000). This hypothesis stems from the fact that hydrothermal systems represent sites where liquid $H_2O$, energy, and dissolved chemicals and nutrients may have been available for extended periods of time. Many deep branching-organisms in the phylogenetic tree are thermophilic (optimum growth temperatures >50 °C) or hyperthermophilic (optimum growth temperatures >80 °C) and would have benefited from hydrothermal environments. While volcanogenic hydrothermal systems would certainly have provided such habitats on the early Earth and other planetary bodies, impact-generated hydrothermal systems would have also been common and widespread at this time and may have provided opportune sites for the growth and colonization of any available and suitable preexisting organisms (Cockell and Lee, 2002). Furthermore, due to increased cratering rates during the first few hundred million years of Solar System history, impact-generated hydrothermal systems created on the surfaces of the inner planets likely outnumbered volcanogenic systems (Kring, 2000).

It is important to note that on planetary bodies whose surfaces are permanently frozen, such as present-day Mars, hydrothermal systems will not only generate thermophilic environments but, as heat tends to decrease exponentially away from the source, volumetrically a much larger volume of rock will be heated to temperatures above the freezing point of $H_2O$ but <50 °C (cf., Schwenzer et al., 2012). This implies that, in terms of spatial extent, the predominant habitat resulting from impact-generated hydrothermal activity on Mars will not be for hyperthermophiles, or even thermophiles, but for mesophiles (i.e., organisms that grow at moderate temperatures between ~20 and 50 °C). Indeed, even if early Mars was always cold and only sometimes "wet" as some have suggested, the interaction of hot impact-generated rocks with ground-ice could still produce groundwater and a subsequent hydrothermal system at the present-day (Barnhart et al., 2010; Ivanov and Pierazzo, 2011; Schwenzer et al., 2012). Thus, if one assumes that there was life on Mars early in its history, then hydrothermal deposits associated with impact craters may provide the best, and most numerous, opportunities for finding preserved evidence for life on Mars.

### 3.1. Is there evidence that impact-generated hydrothermal systems can support life?

We have shown above that impact-generated hydrothermal systems are commonplace on Earth. We now turn our attention to the preservation of biosignatures in these terrestrial systems and the ability of impact-generated hydrothermal systems to support life (Wanger et al., 2008). First, it is important to note that impact-generated hydrothermal systems are understudied from the perspective of biological preservation. To the knowledge of the authors, there have been only four studies reporting fossil evidence of biological activity in such systems: microbial etching of hydrothermal minerals at the Ries impact structure (Glamoclija, 2007); the presence of rod-shaped biomorphs in post-impact hydrothermally altered sediments from the Chesapeake Bay impact structure (Glamoclija et al., 2007); evidence of extracellular polymeric substances in a hydrothermally precipitated calcite vein from the Siljan

impact structure (Hode et al., 2008); and most recently, a report of filamentous 'fossils' hosted in hydrothermally precipitated mineral assemblages within fractured impact breccia from the Dellen impact structure (Lindgren et al., 2010). While these observations are all intriguing, caution is urged as the impact hydrothermal origin of the putative biosignatures and/or their host samples is questionable in some cases. Furthermore, in the above studies much of the evidence rests on limited morphological data and the biogenicity is equivocal. Within the Haughton impact structure, there is chemical evidence of biological activity from sulfur isotopes (Parnell et al., 2010). This work demonstrated extreme sulfur isotopic fractionation in hydrothermal sulfides relative to original sulfate lithologies, much greater than any known abiological kinetic isotope fractionation, thus requiring microbial sulfate reduction by thermophiles throughout the crater (Parnell et al., 2010).

### 3.2. A case study

In this section we present a case study of an intriguing hydrothermal pipe feature within the Haughton impact structure. As noted above, these structures have been interpreted as paleohydrothermal vent deposits (Osinski et al., 2005). The pipe structure in question contains laminated deposits similar in appearance to stromatolites, leading to the question of whether the vent contains fossilized bacterial cells.

#### 3.2.1. Field observations

The exposed portion of the hydrothermal pipe structure is ~40 m wide and 4 m high. The orange–brown outcrop of weathered hydrothermal rock is found within the carbonate target rocks of the Allen Bay Formation (Fig. 3). A sharp contact marks the transition from the Allen Bay Formation rocks to the hydrothermal material. This is evident by the appearance of the laminated texture found in the hydrothermal vent deposit (Fig. 4). Our hypothesis based on field and hand specimen-scale observations was that this laminated unit may be biological in origin. The second, intriguing feature of the hydrothermal pipe was the presence of microbial mats that were observed in a small stream flowing around the base of the outcrop. The mat begins as the stream encounters the weathered hydrothermal material being eroded from the pipe, and extended downstream form the pipe becoming up to 2 mm thick. It was not observed upstream where the water flows through the Allen Bay Formation target rocks.

#### 3.2.2. Laboratory observations

Optical microscopy coupled with X-ray Diffraction (XRD) demonstrated that bands of microcrystalline goethite run through the hydrothermal samples. These are sub-parallel and branched, with widths ranging from 0.1 to 4.7 mm (Fig. 5a and b). The goethite is present as an orange–brown stain on the euhedral dolomite and calcite grains, as well as space filling cement between the grains. The larger patches of cement show growth zoning which conforms to the edges of the surrounding carbonate grains. Some of the carbonate grains exhibit fractures filled with goethite cement. Scanning electron microscopy (SEM) was used to view the textures seen with the optical microscope at a higher resolution. Backscattered electron images show the space filling growth of the goethite cement (Fig. 6a and b).

**Fig. 4.** Hand specimen of a hydrothermally laminated sample from the outcrop in Fig. 7. Centimeter ruler for scale.

#### 3.2.3. Origin of the laminated texture

The laminated texture present in the hydrothermal pipe samples does not appear to be the result of biological activity, even though it possesses a strong resemblance to stratiform stromatolites, such as those known to the Gunflint Iron Formation (Schopf et al., 2007). The hematite banded rocks of the Gunflint Formation contain fossilized cells and have been used as an analog for iron formations on Mars (Schelble et al., 2004). Despite the similarities, the laminations in the hydrothermal rocks in this investigation are composed of goethite cement between euhedral dolomite and minor calcite grains. Secondary calcite crosscuts the goethite bands, indicating that this calcite formed after the goethite was in place. The goethite cement exhibits space filling growth textures, which are visible among the carbonate phases using both

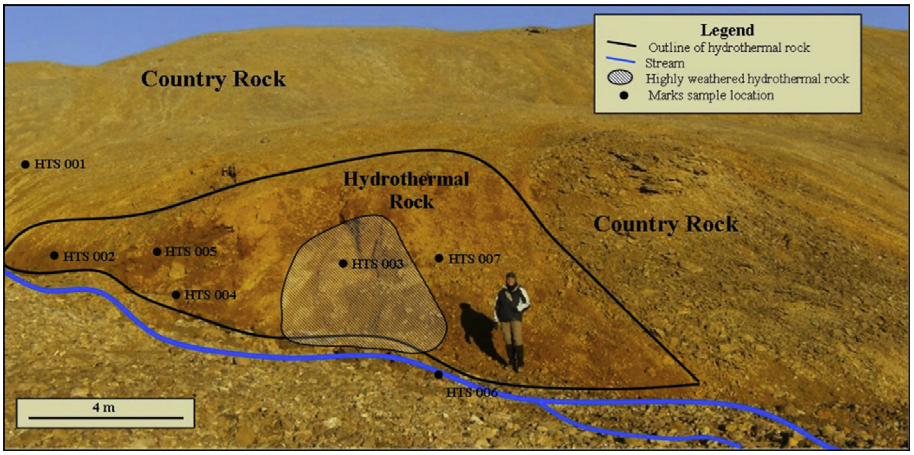


**Fig. 3.** Field photograph of the hydrothermal pipe outcrop at the Haughton impact structure that displays an unusual laminated texture (shown in Fig. 4).

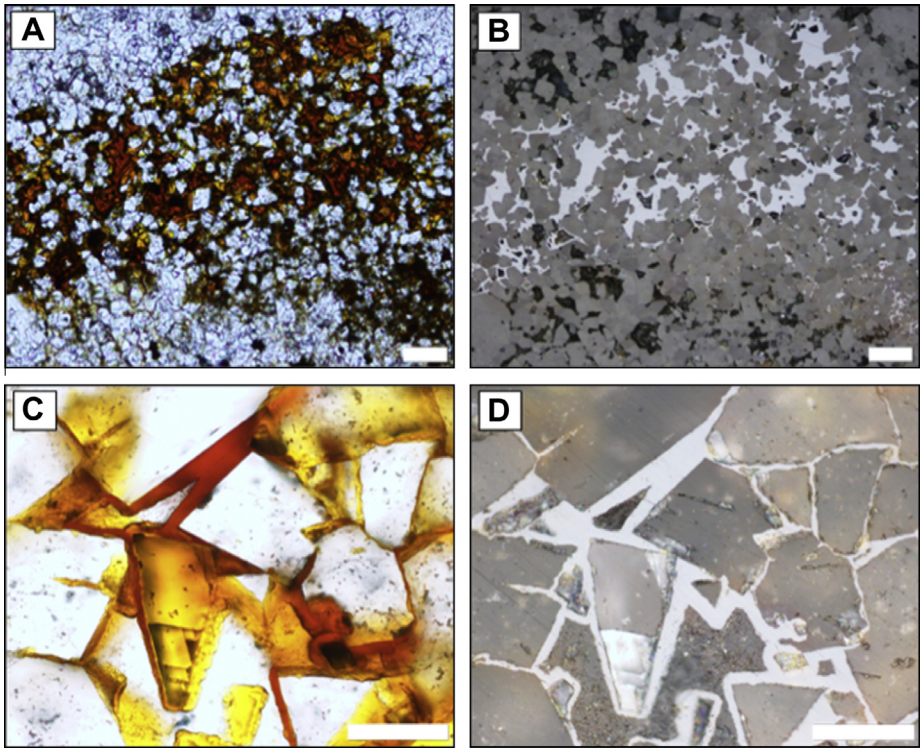


**Fig. 5.** Goethite cement viewed with (a) plane polarized light and (b) reflected light. Goethite cement (orange–brown) between dolomite grains and goethite stain (yellow) on dolomite grains viewed under (c) plane polarized light and (d) reflected light in section HTS 007B. Scale bar equals 50 μm in all images. (For interpretation of the references to color in this figure legend, the reader is referred to the web version of this article.)

light and electron microscopy. This growth texture is usually the result of an abiotic processes (Mohapatra et al., 2007). If microbial life had been present at the time of mineralization, this concentric growth would have presumably coated the cells, resulting in preservation such as that seen in goethite cement at Rio Tínto (Preston et al., 2011). In addition, no evidence of microbial life, such as fossilized bacteria or the presence of biologically precipitated minerals, was detected in the hydrothermal pipe rock samples. The lack of structural biological markers in the hydrothermal pipe rock samples may be an indication that this precipitation occurred at temperatures too high for life to tolerate.

Goethite (FeO(OH)) precipitation from fluids is common following the dissolution of ferrihydrite ($Fe_2O_3{\cdot}0.5H_2O$) (Burlson and Penn, 2006). Because hydrothermal fluids are reducing, both the initial ferrihydrite and the following goethite must have precipitated near surface in order for oxygen to be present. Meteoric waters would provide oxygen when mixed with the upwelling hydrothermal fluids. Iron in the hydrothermal water was likely released through the oxidation of iron sulfides, which was then precipitated as ferrihydrite. Progression of the hydrothermal system would result in dissolution of the ferrihydrite, the products of which were then precipitated as the goethite cement found in the hydrothermal pipe samples studied in this investigation. Goethite precipitation occurs in both acidic and alkaline waters, with optimum precipitation occurring at pH 4 and 12 (Schwertmann and Murad, 1983). No evidence indicates basic fluids in the hydrothermal system at Haughton; however, fluid inclusion and hydrothermal mineral analyses suggest the pH dropped below 7 at the end of the main stage of the hydrothermal system (Osinski et al., 2005). These conditions favor goethite precipitation over hematite, which forms more readily around pH 7–8 (Schwertmann and Murad, 1983). The laminated bands likely formed as a result of the dynamic nature of this system. Changes in the chemistry and flow patterns of the hydrothermal fluids would have occurred as the system continued to cool. In addition, the volume of meteoric waters would change with seasonal precipitation resulting in concentration changes of the dissolved ions within it, altering the mixing ratio between these two fluids. The laminations may represent a cyclical relationship, marking periods during which substantial iron oxide precipitation was favored. The growth zoning, especially evident in SEM images, is common to cavity filling goethite, which crystallizes as an encrusting layer on surrounding grains (Mohapatra et al., 2007).

The ambiguity surrounding the origin of the laminated texture in these deposits of hydrothermal origin at Haughton provides a compelling case for a Mars Sample Return mission. We have shown that biogenicity cannot be determined visually and that laminated textures like this can be misleading. This despite the fact that there is convincing evidence for thermophilic organisms having colonized the hydrothermal system at Haughton (Parnell et al., 2010).

### 3.3. Hydrothermal rock-fed biosphere

Despite the above discussion, there is strong evidence that hydrothermally-altered rocks can help to generate and/or sustain a biosphere for mesophilic organisms. We return now to the microbial mats that were observed in a small stream flowing around the base of the outcrop shown in Fig. 3. Light microscopy was used to characterize the microorganisms in the microbial mat sample (Table 2). In some cases, morphology could be used to identify the organisms. Four genera of cyanobacteria were observed in both the natural microbial mat sample and the enrichments. Three of these, cf. *Limnothrix*, cf. *Oscillatoria*, and cf. *Komvophoron* are filamentous, while cf. *Gloeocapsa* is spherical. All of these cells exhibited autofluorescence at 660 nm, indicative photosynthetic pigments (Fig. 7a and b). The filamentous organisms could also be differentiated based on cell and filament dimensions (Table 2;

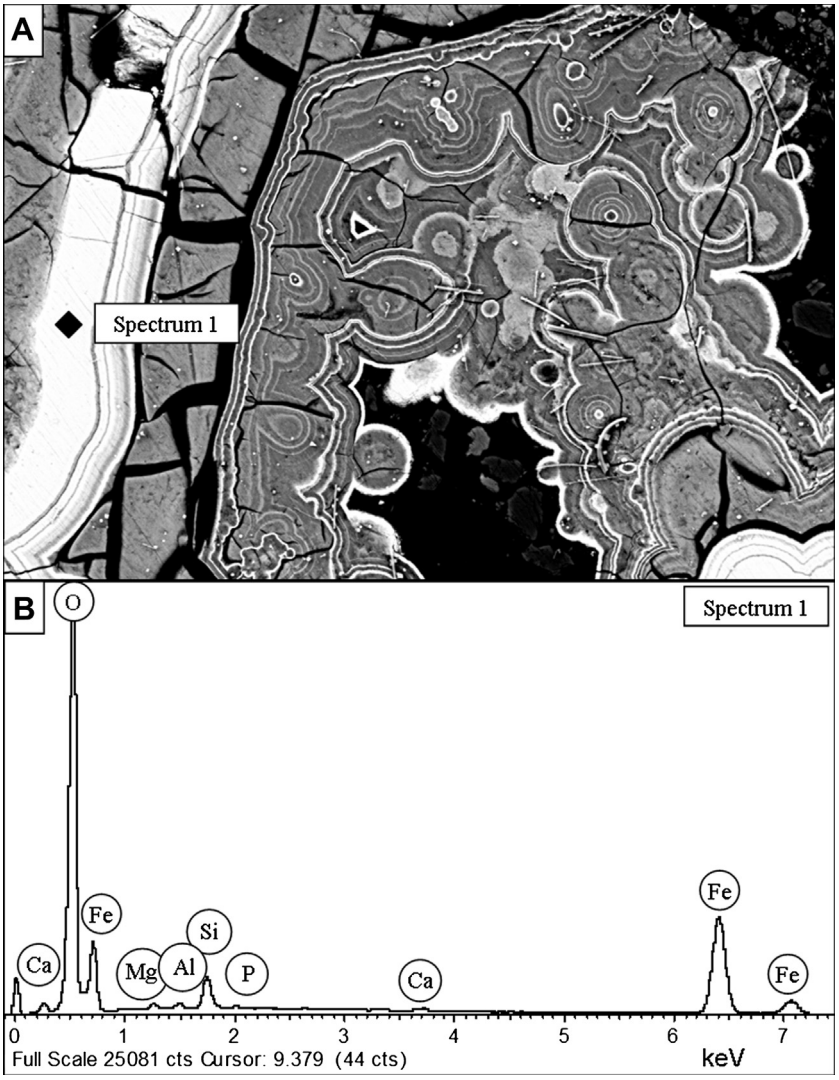


**Fig. 6.** (a) Back scattered electron image showing space filling growth of the goethite (white through dark gray) cement and locations of two EDS spectra; (b) higher magnification view of the goethite cement growth habit shown in (a); (c and d) EDS spectra for points marked in (a). "d" is representative of the chemistry of the entire ringed-growth region of the sections. Alternating zone of high- (bright) and low-atomic mass regions (darker) demonstrate that the goethite contains lighter elements. Scale bar equals 50.0 μm in "a" and 5.00 μm in "b".

Fig. 7d and f). Individuals of cf. *Gloeocapsa* were identified as clusters that exhibited visible hemispherical protoplasts.

Three alga were characterized from the natural microbial mat sample, two of which were diatoms with third being a green alga (Table 2). An unidentified diatom was present as chains of rectangular valves. The second diatom, cf. *Sellaphora*, has a linear valve, with smooth, rounded ends. The third alga present was a spherical green alga with visible chloroplasts. Two protozoa were characterized; however, neither could be identified. Both were highly mobile and observed feeding on the phototrophs present in the natural sample. The first was smooth, spherical, and green due to the presence of phototrophs within. The second was composed of elongated, segmented cells, which tapered at both ends.

Inoculation of microbial mat samples into culture media prepared with the sterilized hydrothermal rock, weathered hydrothermal material, and the solutions produced by the sulfuric acid digestion of both unweathered and weathered hydrothermal pipe in distilled water ($dH_2O$) supported growth of this complex biosphere. No growth occurred in sterile $dH_2O$. Growth of the mat in BG-11 medium, containing high levels of nitrogen and phosphorus resulted in abundant growth. This data is consistent with the absence of microbial mats in the surrounding terrain and their concentration downstream of the hydrothermal pipe structure in Fig. 3.

In summary, this case study shows that hydrothermally altered and precipitated rocks can provide nutrients capable of sustaining a biosphere long after hydrothermal activity has ceased. This is important in polar desert environments like the Haughton impact structure on Devon Island where nutrients are limited (Cockell et al., 2001), and may also be relevant for Mars. Similarly, ancient primary hydrothermal minerals (Parnell et al., 2004) have also been demonstrated to provide habitats for present-day microbial life and the same can potentially be said for secondary assemblages formed by the alteration of primary hydrothermal minerals (Izawa et al., 2011).

## 4. Potential for impact-generated hydrothermal activity on Mars

The possibility of impact-generated hydrothermal systems on Mars was first proposed and discussed in detail by Newsom

**Table 2**
Morphological characteristics of microorganisms observed in the natural microbial mat sample and the cultured enrichments.

| Domain | Group | Cell characteristics | Cell size (μm) | Cell arrangement | Color | Visible sheath | Visible motility | Identification |
|---|---|---|---|---|---|---|---|---|
| Bacteria | Cyanobacteria | Rectangular, longer than wide, no constriction at cross-walls, gas vesicles present | 2–6 | Filamentous | Blue–green | No | No | cf. *Limnothrix* |
| | | Discoid cells, wider than long, no constrictions at cross-walls | 8–12 | Filamentous | Blue–green | No | Yes | cf. *Oscillatoria* |
| | | Barrel shaped, longer than wide, constriction at cross-walls | 4–8 | Filamentous | Green | No | No | cf. *Komvophoron* |
| | | Spherical, protoplasts visible, no gas vesicles | 5–8 | Clusters | Green | Yes | No | cf. *Gloeocapsa* |
| Eukarya | Algae | Spherical, multiple chloroplasts per cell, no visible motility structures | 4–5 | Clusters | Green | N/A | No | Unknown |
| | | Linear valve with smoothly rounded poles | 25 | Individual | Yellow to colorless | N/A | Yes | cf. *Sellaphora* |
| | | Angular valves, width greater than length, slightly convex along the width of the valves | 10–20 | Chains | Green to colorless | N/A | Yes | Unknown |
| | Protista | Spherical to slightly elongated, highly mobile, no visible flagella or depression in the cell wall marking a flagellar base | 20–25 | Individual | Green | N/A | Yes | Protozoa |
| | | Elongated, segmented cell, both ends taper, visible sweeping structures for feeding, movement by cell contraction and elongation | 150–200 | Individual | Colorless, digested phototrophs visible | N/A | Yes | Protozoa |

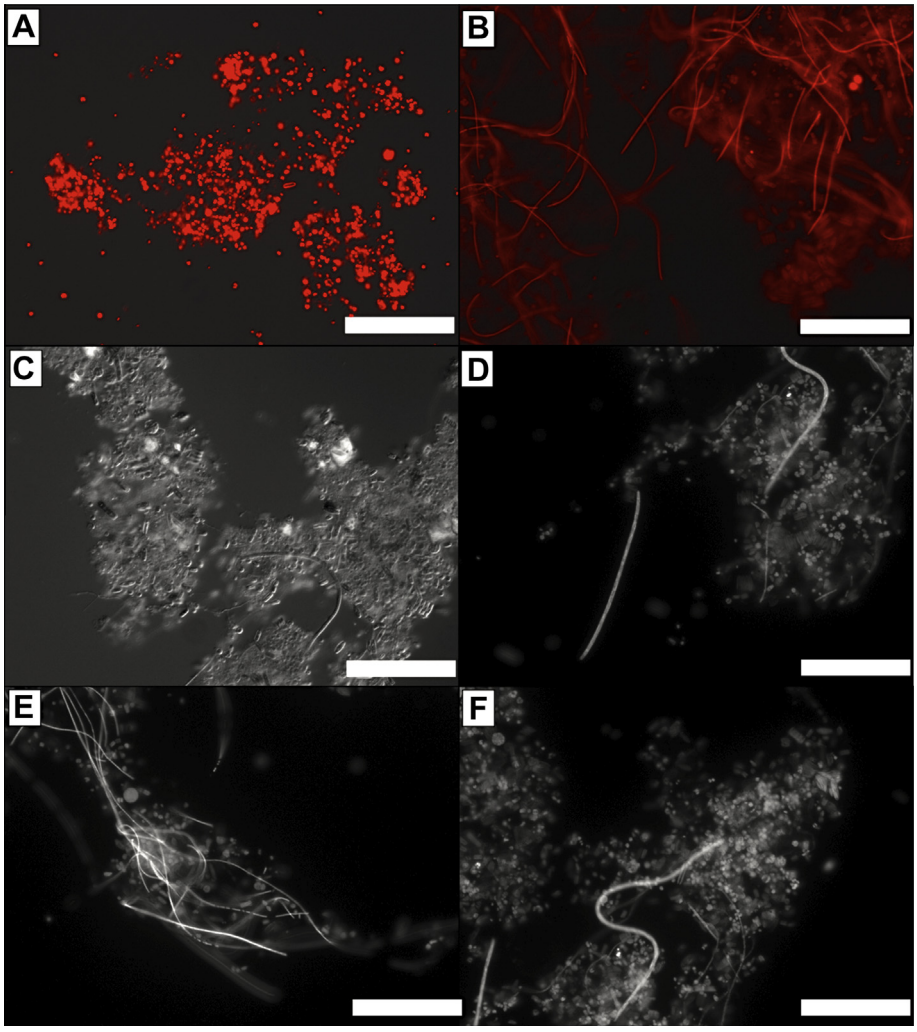


**Fig. 7.** Autofluorescence of (a) spherical algae and (b) filamentous cyanobacteria. (c) Differential Interference Contrast (DIC) image of microbial diversity and cell arrangement. (d–f) Autofluorescence of cyanobacteria filaments of varying thickness. Scale bar equals 100 μm in all images.

(1980). Little work was then conducted on this topic for a number of years. More recently, a number of publications have contributed to our understanding of the potential for the generation of hydrothermal systems within martian impact craters. Modeling of craters of various sizes and using various codes has shown that impact-generated hydrothermal systems on Mars should be generated and be active on timescales of up to several hundreds of thousands of years producing mineral assemblages consistent with

those documented from orbiting spacecraft (Rathbun and Squyres, 2002; Abramov and Kring, 2005; Schwenzer and Kring, 2009). Given the earlier discussions concerning the astrobiological potential for hydrothermal systems in general, this should be of prime interest for future missions aiming to seek out evidence for past life on Mars. As we have shown above, studies of impact craters on Earth can provide the necessary ground truth for models and provide information as to the expected distribution and location of impact-generated hydrothermal deposits. One of the most important observations is that hydrothermal alteration in craters on Earth is concentrated into several distinct settings around an impact crater (Fig. 1). Given the pervasive occurrence of impact-generated hydrothermal systems (and their associated alteration) on Earth, it is logical to infer that similar processes have been active on Mars.

### 4.1. Occurrence of hydrated phases on Mars

Results from the Observatoire pour la Mineralogie, l'Eau, les Glaces et l'Activitié (OMEGA) and Compact Reconnaissance Imaging Spectrometer for Mars (CRISM) VNIR spectrometers, onboard the Mars Express (MEx) and the Mars Reconnaissance Orbiters (MRO), respectively (Bibring et al., 2006; Murchie et al., 2009a), continue to reveal the presence of abundant hydrated phases (both silicates and sulfates) on the martian surface. The results of a detailed analysis of the occurrence of hydrated silicate phases (particularly, clay minerals, zeolites, and hydrated silicate glasses) indicate that many of these phases are associated with the heavily cratered southern highlands of Mars (Mustard et al., 2008; Ehlmann et al., 2011), and northern lowland exposures, which are exclusively in impact craters (Carter et al., 2010). Global mapping by Carter et al. (2011b) using a mosaic of the OMEGA data and 1680 individual high-resolution observations from CRISM indicate that localized hydrated silicates on Mars are dominated by mixed layered Fe–Mg rich smectites/chlorites with ~70% correlating specifically with impact craters. An independent study by Ehlmann et al. (2011) of 629 CRISM high-resolution observations generally agrees with the findings of Carter et al. (2011a,b), but classifies both the crater-exposed and the less common tectonic-exposed occurrences together as "crustal clays". The correlation between hydrated silicates and impact craters suggests that detailed studies are needed to understand the origin of these materials, since they can be either pre-, syn- (i.e., impact-generated) or post-impact in origin, or some combination thereof.

### 4.2. Examples of pre- and post-impact hydrated phases on Mars

There continues to be much discussion in the community regarding the origin of hydrated silicates that are associated with impact craters (e.g., Mustard et al., 2009; Carter et al., 2011a,b; Ehlmann et al., 2011). It is important to note before proceeding further that there are three possible associations of hydrated phases with impact craters. Pre-impact hydrated silicates are simply those that existed in the target prior to the uplift and/or excavation by an impact event. A post-impact origin refers specifically to eroded and redeposited altered materials that are not related to the formation of the exposing/host crater. Given the complexity of Noachian-aged surfaces, it should be noted that these two cases may still include impactites from other craters or large impact basins, but are distinct in the sense that the origin is not specifically tied to the crater in which these deposits or formations are exposed. The syn-impact or impact-generated origin of hydrated phases is discussed in the next section.

There are numerous examples of pre-impact clays associated with simple craters on Mars (Fig. 8). Unlike complex craters, simple craters are generally expected to have minimal impact-generated alteration effects (see Table 1) due to smaller volumes of impact melt deposits and the lack of a central uplift. As such, they represent the least ambiguous examples of case where the crater "resamples" or excavates preexisting clays. Fig. 8a shows an excellent example where an unnamed simple crater in Tyrrhena Terra uplifted and exposed the clay-rich materials within the rim/wall rock as well as excavating these materials and incorporating them into the ejecta blanket (Carter et al., 2011a). The observation of a possible clay unit in the most distal portion of the ejecta blanket, may indicate that clay-rich materials were excavated from a stratigraphically shallow portion of the target rock. Similar spectral signatures correlated can also be observed at some complex craters (Fig. 8b); however, with increasing melt deposition within the ejecta blanket as crater diameter increases (Osinski et al., 2011), some of the altered materials in complex crater ejecta can be overprinted by impact-generated alteration. Generally, the ability to distinguish pre-impact and impact-generated alteration materials becomes more complicated with complex craters, particularly in the area of the central uplift.

In terms of post-impact clays, there are numerous good examples of these occurrences in the current literature (e.g., Holden intra-crater fill deposits (Grant et al., 2008), Eberswalde, Jezero (Ehlmann et al., 2009), and Gale crater (Milliken et al., 2010)). In general, post-impact clays show clear associations between spectral and morphologic units that are clearly post-impact in origin (e.g., layered deposits, deltaic deposits, channel deposits, etc.). However, there is some ambiguity in the case of infilled or degraded craters with respect to distinguishing impact-generated alteration from pre- and post-impact. It is outside the scope of the current paper to address all these issues in detail, but we suggest here to proceed with caution when trying to determine the origin of alteration signatures on the crater-floor or superimposed on crater central uplifts in degraded craters.

### 4.3. Examples for impact-generated hydrated phases on Mars

To date, observational evidence for impact-generated hydrothermal activity on Mars is scarce. Detailed studies using CRISM and High Resolution Imaging Science Experiment (HiRISE) data sets have been conducted, but due to the time consuming nature of the work it has only accomplished for a handful of martian craters. Three possible examples of impact-generated alteration from Toro and Holden Craters are summarized and described below. The first and less ambiguous example is Toro Crater. Marzo et al. (2010) reported two compelling morphologic features at Toro, one of which correlates specifically with a hydration signature in what are interpreted to be crater-floor impact melt-bearing deposits. Putative hydrothermal mounds were noted to occur only within the confines of the central uplift complex where deposits consistent with impact melt deposits were observed to be sparse and bedrock or breccias were exposed. Unfortunately, these mounds are quite small (the largest in Toro Crater is ~150 m in size) and their spectral characteristics are difficult to isolate in the CRISM data sets. However, building on the Marzo et al. (2010) study, we have recognized these features at other impact craters on Mars (e.g., Fig. 9). Therefore, they do not represent a unique occurrence in Toro, nor are they consistent with unusual erosional remnants, as previously discussed. Given that erosion from crater to crater across Mars is not likely to be the same, the repeat occurrence of the mound morphology described by Marzo et al. (2010) within the central uplift complex of other martian craters are not easily explained as erosional remnants.

The most compelling evidence for impact-generated alteration at Toro manifests as light-toned fractures on the crater floor, which are interpreted to cross-cut the impact-melt bearing crater fill deposits (Marzo et al., 2010). Hydration, specifically the presence of bound water, represented by the CRISM 1900R band parameter

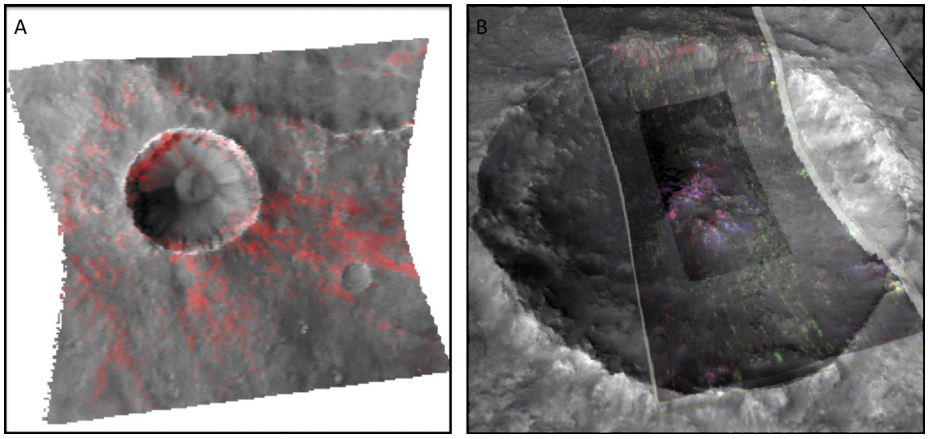


**Fig. 8.** CRISM observations of excavated versus impact-induced hydrated silicates. (a) CRISM Full-Resolution Targeted (FRT) with a BD2300 spectral parameter superimposed on the 1.3 μm IR brightness image. The BD2300 spectral parameter indicates the presence of a 2.3 μm absorption feature consistent with the presence of Fe–Mg rich clays. The crater is ~5-km in diameter. (b) This examples shows a visible/spectral composite of CRISM "phyllosilicate" spectral parameter color composite overlain on CTX and the MOLA MEGDR DEM (10× VE) of a unnamed ~22-km crater located ~40 km east of Toro Crater in Syrtis Major. Spectral signatures, consistent with the presence of Fe–Mg (red) and Al (green), can be observed in the wall-terrace region as well as the ejecta blanket. HiRISE observations of areas of additional hydration signatures (blue and magenta) in the central uplift possibly suggest excavated altered materials (e.g., large altered megablocks) that may be preexisting but also possesses an overprinting by impact-induced hydrothermal activity. Image credits: NASA/JPL/APL/MSSS/ASU. (For interpretation of the references to color in this figure legend, the reader is referred to the web version of this article.)

spectral index image (Murchie et al., 2009b) correlates specifically with the appearance of these light-toned fractures and is completely absent in the same contiguous unit of the crater-fill deposits where the light-toned fractures are absent (Fig. 10).

Our last example involves martian megabreccias that were discovered within HiRISE images of Holden Crater (Grant et al., 2008). The megabrecccias within Holden Crater are unique in that they are interpreted to represent sub-crater floor deposits that were exposed when Uzboi Valles extensively eroded through the ejecta and southwest rim/terraces of Holden Crater (Tornabene et al., 2009). Close inspection of the Holden megabreccias indicate that the CRISM alteration signatures occur almost exclusively between the unaltered mafic to ultramafic megaclasts (Fig. 11). Although sampling of preexisting alteration phases is also possible for Holden Crater megabreccias, the lack of alteration within the largest megablocks and the pervasive alteration observed specifically within the matrix is highly suggestive of impact-generated alteration produced by the Holden-forming event (cf., Tornabene et al., 2009).

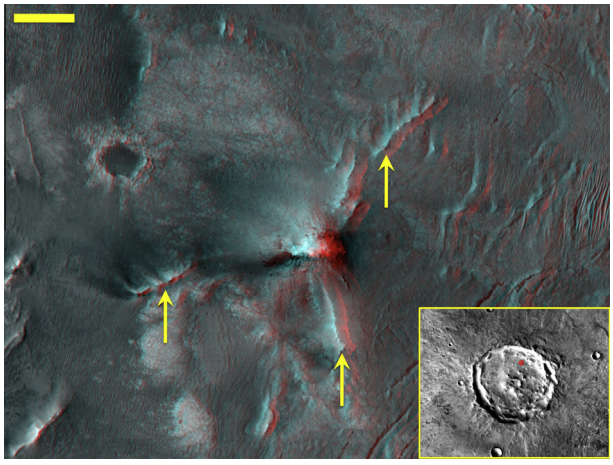

**Fig. 9.** This HiRISE stereo anaglyph (PSP_006607_007108_1985) shows and example of a possible hydrothermal mound in an unnamed ~32-km crater, ~350 km away from Toro Crater. The mound is morphologically identical to those observed in Toro Crater (see Fig. 8 in Marzo et al. (2010)). This mound is an archetype example in that it possesses all of the features outlined in Marzo et al. (2010), including an excellent set of multiple light-toned ridges that may represent mineralized conduits that once fed the mound. Scale bar: ~30 m. Image credits: NASA/JPL/UA/ASU.

### 4.4. Generation of surface discharges?

Of particular interest for astrobiology is the potential for the generation of surficial hot springs around the periphery of complex impact craters, as discovered at the Haughton structure (Osinski et al., 2001; Osinski et al., 2005). Might impact-generated hydrothermal systems on Mars also be located predominantly in the peripheral zones of craters in the form of hydrothermal vents? An explanation of the close spatial association of many martian small valley networks and channels with the rims and walls of impact craters was indeed proposed by invoking the interaction of ground ice and hydrothermal systems (Brackenridge et al., 1985). Regardless of the fact that the model of Brackenridge et al. (1985) does not take into account the complicated faulting relationships present around the periphery of large complex impact craters on Mars, the hypothesis is that hydrothermal activity would have resulted in localized melting of ice, thus spawning networks of meltwater channels and eventually small valley systems. Recent modeling of hydrothermal systems that takes into account freezing and the starting conditions for impacts into $H_2O$-rich targets show that hydrothermal systems with surface discharges are possible on timescales of $10^3$–$10^5$ years (Barnhart et al., 2010; Ivanov and Pierazzo, 2011) and in craters as small as ~5–20 km (Schwenzer et al., 2012). Observations of channels emanating from the impact ejecta blankets at the Hale (Jones et al., 2011) and Lyot (Harrison et al., 2010) also provide intriguing support for this hypothesis.

### 4.5. Importance of impact crater lakes

As discussed above, observations of impact craters on Earth appear to demonstrate the critical role of impact crater lakes in determining the longevity and size of impact hydrothermal systems. A comparison of the hydrothermal systems that developed within the Ries and Haughton structures suggests that the presence of an impact crater lake immediately post-impact is required for the generation of a large hydrothermal system capable of

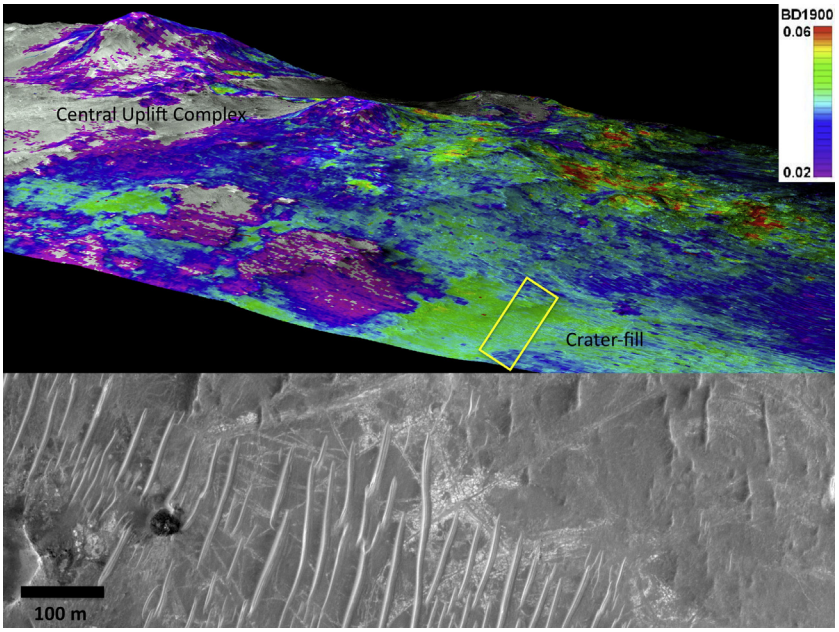


**Fig. 10.** CRISM and HiRISE observations of the crater-fill and central uplift complex of Toro Crater, Syrtis Major, Mars. (a) CRISM hydration parameter (1900R) superimposed on a HiRISE red mosaic image draped on a stereo-derived Digital Terrain Model (DTM). The CRISM 1900R hydration parameter (Murchie et al., 2009a,b) correlates with the observation of light-toned fractures that are interpreted to cross-cut the impact melt-bearing deposits mapped by Marzo et al. (2010). The presence of a ~1.9 μm feature indicates the presence of mineral or amorphous phases (e.g., glass) with bounded $H_2O$ within their molecular structures. The width of the HiRISE image is ~6 km. (b) A HiRISE subimage close-up of the area outlined in the box in (a). Light-toned fractures are not observed within the crater-fill where hydration is weak. Image credits: NASA/JPL/APL/UA. (For interpretation of the references to color in this figure legend, the reader is referred to the web version of this article.)

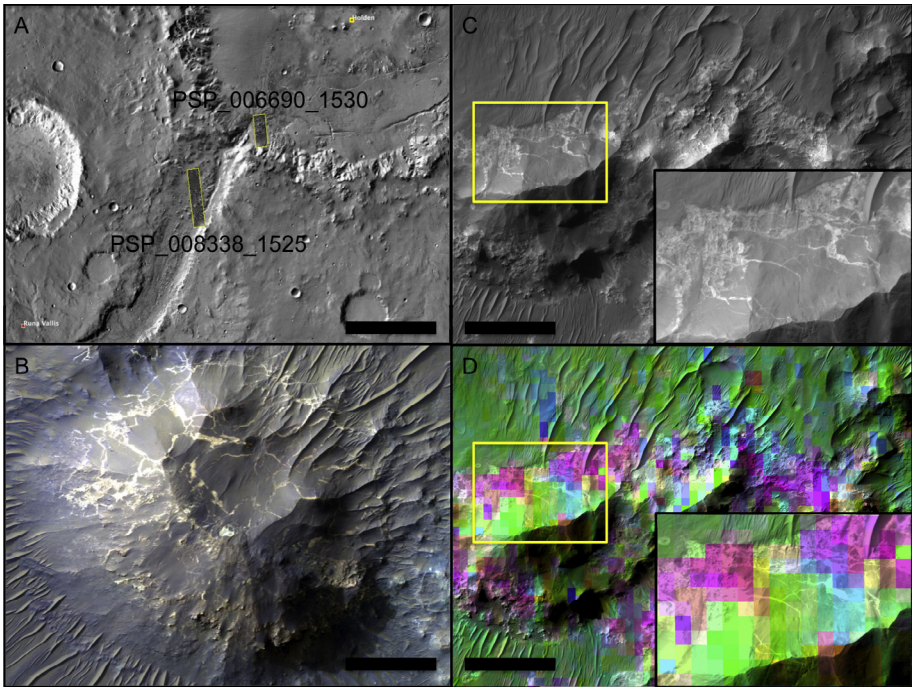


**Fig. 11.** Fractured basement (possible parautochthonous megabreccias) of the Holden impact crater as seen exposed in Uzboi Valles, Mars. (a) Location and context map for the HiRISE/CRISM observations shown in (b and c). Scale bar: ~50 km. (b) An HiRISE infrared color (PSP_008338_1525) subset showing an example of an outcrop of fractured basement in Uzboi Valles that lies ~30 km away from Holden rim and ~1.5 km deep beneath the Holden crater rim (Tornabene et al., 2009). Scale bar: ~250 m. (c) HiRISE ~25-cm/pixel red mosaic subimage for comparison with (d) a HiRISE–CRISM composite consisting of a 2300-2100-1900R band parameter color composite (see Murchie et al., 2009a,b) representing unaltered mafic rocks in green and altered materials in magenta, cyan and yellow. Note the correlation between the light-toned fractures and the alteration signature associated with a ~2.3 μm and ~1.9 μm features consistent with a Fe–Mg-bearing clay with bound $H_2O$, respectively (c.f., c and d). Dark-toned bedrock appears to consist predominately of unaltered mafic materials. If light-toned fractures are associated with the formation of Holden Crater, then the alteration observed here may be related to an impact-induced hydrothermal system. These observations (see a and PSP_006690_1530) are consistent with deeply incised terrace blocks just within the Holden Crater interior where Uzboi Vallis has eroded into the crater (Tornabene et al., 2009). (c and d) Scale bar: ~200 m. (For interpretation of the references to color in this figure legend, the reader is referred to the web version of this article.)

pervasively altering large volumes of rock. When absent, alteration may be more short-lived and confined to a limited extent (e.g., Haughton). This must be considered when invoking models for impact-generated hydrothermal systems on Mars.

In a review of 179 impact crater paleolakes on Mars, Cabrol and Grin (1999) documented a main concentration of crater lakes in the cratered uplands and associated with abundant populations of fluvial valley networks. These authors also noted that while most of the craters studied were of Noachian in age, the paleolakes were predominantly of early to Late Hesperian age, with several clear examples of deposition during the Amazonian. However, we may not expect every impact throughout the history of Mars to have generated a hydrothermal system because the paleoenvironment and target setting plays a critical role in determining if such systems would have developed.

Conversely, the generation of impact-generated hydrothermal systems has important implications for the development and longevity of crater lakes. Specifically, modeling suggests that the lifetime of crater lakes can be extended by tens of millions of years by the presence of such systems and that they can remain partially unfrozen with a cap of ice for similar time periods (Newsom et al., 1996).

## 5. Summary

Consideration of the impact cratering record on Earth suggests that hydrothermal activity will be commonplace after the impact of an asteroid or comet into $H_2O$-rich planetary surfaces. Hydrothermal systems represent sites where water, heat, dissolved chemicals and nutrients may have been available for extended periods of time. As such, these hydrothermal systems are prime locations suitable for colonization by thermophilic microorganisms. Imaging of the surface of Mars by several generations of orbiting spacecraft reveals that water once flowed and probably ponded over the surface of the planet earlier in its history. Since then, however, the picture of Mars is of a dry, cold inhospitable planet. However, impact cratering is a ubiquitous geological process that has occurred since the birth of the Solar System and which will continue to occur to its very end. It is, therefore, a distinct possibility that the interaction of hot impact-generated rocks with ground-ice could produce liquid groundwater even under present climatic conditions on Mars. Could life, therefore, still exist somewhere below the martian surface? Future robotic and/or manned missions to Mars are required to answer this fundamental question.

We have shown that hydrothermal deposits may be found in six main sites within an impact crater (Figs. 1 and 2). Studies of terrestrial craters reveal the importance of impact-generated fault systems in governing the location and nature of post-impact hydrothermal activity. These fault systems are thought to have acted as fluid pathways, enabling hot fluids and steam to travel along them. Of the various types and locations of hydrothermal deposits, we suggest that fossil hydrothermal vents offer the best targets for searching for extinct or extant life on Mars. It is our hope that this contribution will focus the search to areas around impact craters where hydrothermal systems may have once existed.

## Acknowledgments

G.R.O. is supported by the Natural Sciences and Engineering Research Council of Canada (NSERC) Industrial Research Chair in Planetary Geology sponsored by MDA Space Missions and the Canadian Space Agency (CSA). Funding from the NSERC Discovery Grant, CSA Canadian Analogue Research Network (CARN), the Polar Continental Shelf Project (PSC), and Northern Scientific Training Program (NSTP) programs to various authors provided the resources to carry out field and laboratory-based studies of the hydrothermal systems at the Haughton, Ries, and Sudbury impact structures and is gratefully acknowledged. We thank Susanne Schwenzer and an anonymous reviewer for their detailed and constructive reviews.

## References

Abramov, O., Kring, D.A., 2004. Numerical modeling of an impact-induced hydrothermal system at the Sudbury crater. J. Geophys. Res., 109. http://dx.doi.org/10.1029/2003JE002213.

Abramov, O., Kring, D.A., 2005. Impact-induced hydrothermal activity on early Mars. J. Geophys. Res., 110. http://dx.doi.org/10.1029/2005JE002453.

Abramov, O., Kring, D.A., 2007. Numerical modeling of impact-induced hydrothermal activity at the Chicxulub crater. Meteorit. Planet. Sci. 42, 93–112.

Ames, D.E., Watkinson, D.H., Parrish, R.R., 1998. Dating of a regional hydrothermal system induced by the 1850 Ma Sudbury impact event. Geology 26, 447–450.

Ames, D.E., Watkinson, D.H., Parrish, R.R., 2006. Impact-generated hydrothermal system – Constraints from the large Paleoproterozoic Sudbury Crater, Canada. In: Cockell, C.S., Gilmour, I., Koeberl, C. (Eds.), Biological Processes Associated with Impact Events. Springer, New Work, pp. 55–100.

Ames, D.E., Davidson, A., Wodicka, N., 2008. Geology of the giant Sudbury polymetallic mining camp, Ontario, Canada. Econ. Geol. 103, 1057–1077.

Arp, G., 1995. Lacustrine bioherms, spring mounds, and marginal carbonates of the Ries Impact Crater (Miocene, Southern Germany). Facies 33, 35–89.

Barnhart, C.J., Nimmo, F., Travis, B.J., 2010. Martian post-impact hydrothermal systems incorporating freezing. Icarus 208, 101–117.

Bibring, J.-P. et al., 2006. Global mineralogical and aqueous Mars history derived from OMEGA/Mars Express data. Science 312, 400–404.

Brackenridge, G.R., Newsom, H.E., Baker, V.R., 1985. Ancient hot springs on Mars: Origins and paleoenvironmental significance of small martian valleys. Geology 13, 859–862.

Burlson, D.J., Penn, R.L., 2006. Two-step growth of goethite from ferrihydrite. Langmuir 22, 402–409.

Cabrol, N.A., Grin, E.A., 1999. Distribution, classification, and ages of martian impact crater lakes. Icarus 142, 160–172.

Cabrol, N.A., Grin, E.A., Newsom, H.E., Landheim, R., Mckay, C.P., 1999. Hydrogeologic evolution of Gale crater and its relevance to the exobiological exploration of Mars. Icarus 139, 235–245.

Carr, M.H., 1996. Water on Mars. Oxford University Press, New York, pp. 229.

Carr, M.H., 2006. The Surface of Mars. Cambridge University Press, Cambridge, pp. 307.

Carter, J., Poulet, F., Bibring, J.P., Murchie, S., 2010. Detection of hydrated silicates in crustal outcrops in the Northern plains of Mars. Science 328, 1682–1686.

Carter, J., Poulet, F., Loizeau, D., Bibring, J.P., Murchie, S., 2011a. Impact craters as probes to investigate the upper crustal hydrous mineralogy on Mars. Lunar Planet. Sci. 42. 2619 pdf.

Carter, J., Poulet, F., Ody, A., Bibring, J.P., Murchie, S., 2011b. Global distribution, composition and setting of hydrous minerals on Mars: A reappraisal. Lunar Planet. Sci. 42. 2593 pdf.

Cockell, C.S., Lee, P., 2002. The biology of impact craters – A review. Biol. Rev. 77, 279–310.

Cockell, C.S., Lee, P., Schuerger, A.C., Hidalgo, L., Jones, J.A., Stokes, M.D., 2001. Microbiology and vegetation of micro-oases and polar desert, Haughton impact crater, Devon Island, Nunavut, Canada. Arctic Antarct. Alpine Res. 33, 306–318.

Cockell, C.S., Osinski, G.R., Banerjee, N.R., Howard, K.T., Gilmour, I., Watson, J.S., 2010. The microbe–mineral environment and gypsum neogenesis in a weathered polar evaporite. Geobiology 8, 293–308.

Ehlmann, B.L. et al., 2009. Identification of hydrated silicate minerals on Mars using MRO-CRISM: Geologic context near Nili Fossae and implications for aqueous alteration. J. Geophys. Res., 114. http://dx.doi.org/10.1029/2009JE003339.

Ehlmann, B.L. et al., 2011. Subsurface water and clay mineral formation during the early history of Mars. Nature 479, 53–60.

Farmer, J.D., 2000. Hydrothermal systems: Doorways to early biosphere evolution. GSA Today 10, 1–9.

Glamoclija, M., 2007. Fossil Microbial Signatures from Impact Induced Hydrothermal Settings; Preliminary SEM Results from the ICDP-USGS Chesapeake Bay Impact Structures Drilling Project. Geological Society of America Abstracts with Programs.

Glamoclija, M., Schieber, J., Reimold, W.U., 2007. Microbial signatures from impact-induced hydrothermal settings of the Ries crater, Germany: A preliminary SEM study. Lunar Planet. Sci. 38. 1989 pdf.

Grant, J.A. et al., 2008. HiRISE imaging of impact megabreccia and sub-meter aqueous strata in Holden Crater, Mars. Geology 36, 195–198.

Grieve, R.A.F., 2005. Economic natural resource deposits at terrestrial impact structures. In: McDonald, I., Boyce, A.J., Butler, I.B., Herrington, R.J., Polya, D.A. (Eds.), Geological Society, London, Special Publications, pp. 1–29.

Grieve, R.A.F., Cintala, M.J., 1992. An analysis of differential impact melt-crater scaling and implications for the terrestrial impact record. Meteoritics 27, 526–538.

Grieve, R.A.F., Therriault, A., 2004. Observations at terrestrial impact structures: Their utility in constraining crater formation. Meteorit. Planet. Sci. 39, 199–216.

Hagerty, J.J., Newsom, H.E., 2003. Hydrothermal alteration at the Lonar Lake impact structure, India: Implications for impact cratering on Mars. Meteorit. Planet. Sci. 38, 365–381.

Harrison, T.N. et al., 2010. Impact-induced overland fluid flow and channelized erosion at Lyot Crater, Mars. Geophys. Res. Lett., 37. http://dx.doi.org/10.1029/2010GL045074.
Hode, T., Von Dalwigk, I., Broman, C., 2003. A hydrothermal system associated with the Siljan impact structure, Sweden – Implications for the search for fossil life on Mars. Astrobiology 3, 271–289.
Hode, T., Cady, S.L., Von Dalwigk, I., Kristiansson, P., 2008. Evidence of ancient microbial life in an impact structure and its implications for astrobiology – A case study. In: Seckbach, J., Walsh, M. (Eds.), From Fossils to Astrobiology: Records of Life on Earth and the search for Extraterrestrial Biosignatures. Springer, Berlin, pp. 249–273.
Hörz, F., 1982. Ejecta of the Ries crater, Germany. In: Silver, L.T., Schultz, P.H. (Eds.), Geological Implications of Impacts of Large Asteroids and Comets on the Earth. Geological Society of America Special Paper 190. Geological Society of America, Boulder, Colorado, USA, pp. 39–55.
Ivanov, B.A., Pierazzo, E., 2011. Impact cratering in $H_2O$-bearing targets on Mars: Thermal field under craters as starting conditions for hydrothermal activity. Meteorit. Planet. Sci. 46, 601–619.
Izawa, M.R.M., Banerjee, N.R., Osinski, G.R., Flemming, R.L., Parnell, J., Cockell, C.S., 2011. Weathering of post-impact hydrothermal deposits from the Haughton impact structure: Implications for microbial colonization and biosignature preservation. Astrobiology 11, 537–550.
Jõeleht, A., Kirsimäe, K., Plado, J., Versh, E., Ivanov, B.A., 2005. Cooling of the Kardla impact crater: II. Impact and geothermal modeling. Meteorit. Planet. Sci. 40, 21–33.
Jolley, D., Gilmour, I., Gurov, E., Kelley, S., Watson, J., 2010. Two large meteorite impacts at the Cretaceous–Paleogene boundary. Geology 38, 835–838.
Jones, A.P., Mcewen, A.S., Tornabene, L.L., Baker, V.R., Melosh, H.J., Berman, D.C., 2011. A geomorphic analysis of Hale crater, Mars: The effects of impact into ice-rich crust. Icarus 211, 259–272.
Kenkmann, T., Von Dalwigk, I., 2000. Radial transpression ridges: A new structural feature of complex impact craters. Meteorit. Planet. Sci. 35, 1189–1201.
Kring, D.A., 2000. Impact events and their effect on the origin, evolution, and distribution of life. GSA Today 10, 1–7.
Lindgren, P., Ivarsson, M., Neubeck, A., Broman, C., Henkel, H., Holm, N.G., 2010. Putative fossil life in a hydrothermal system of the Dellen impact structure, Sweden. Int. J. Astrobiol. 9, 137–146.
Marzo, G.A., Davila, A.F., Tornabene, L.L., Dohm, J.M., Fairèn, A.G., Gross, C., Kneissl, T., Bishop, J.L., Roush, T.L., Mckay, C.P., 2010. Evidence for Hesperian impact-induced hydrothermalism on Mars. Icarus 208, 667–683.
McCarville, P., Crossey, L.J., 1996. Post-impact hydrothermal alteration of the Manson impact structure. In: Koeberl, C., Anderson, R.R. (Eds.), The Manson Impact Structure, Iowa: Anatomy of an Impact Crater. Geological Society of America Special Paper 302. Geological Society of America, Boulder, pp. 347–376.
Melosh, H.J., 1989. Impact Cratering: A Geologic Process. Oxford University Press, New York, pp. 245.
Milliken, R.E., Grotzinger, J.P., Thomson, B.J., 2010. Paleoclimate of Mars as captured by the stratigraphic record in Gale crater. Geophys. Res. Lett., 37. http://dx.doi.org/10.1029/2009GL041870.
Mohapatra, B.K., Jena, S., Mahanta, K., Mishr, P., 2007. Goethite morphology and composition in banded iron formation, Orissa, India. Resour. Geol. 58, 325–332.
Murchie, S.L. et al., 2009a. A synthesis of martian aqueous mineralogy after 1 Mars year of observations from the Mars Reconnaissance Orbiter. J. Geophys. Res., 114. http://dx.doi.org/10.1029/2009je003342.
Murchie, S.L. et al., 2009b. Compact Reconnaissance Imaging Spectrometer for Mars investigation and data set from the Mars Reconnaissance Orbiter's primary science phase. J. Geophys. Res., 114. http://dx.doi.org/10.1029/2009je003344.
Mustard, J.F. et al., 2008. Hydrated silicate minerals on Mars observed by the Mars Reconnaissance Orbiter CRISM instrument. Nature 454, 305–309.
Mustard, J.F. et al., 2009. Composition, morphology, and stratigraphy of Noachian crust around the Isidis basin. J. Geophys. Res. – Solid Earth Planets, 114. http://dx.doi.org/10.1029/2009JE003349.
Muttik, N., Kirsimae, K., Vennemann, T.W., 2010. Stable isotope composition of smectite in suevites at the Ries crater, Germany: Implications for hydrous alteration of impactites. Earth Planet. Sci. Lett. 299, 190–195.
Naumov, M.V., 2002. Impact-generated hydrothermal systems: Data from Popigai, Kara, and Puchezh-Katunki impact structures. In: Plado, J., Pesonen, L.J. (Eds.), Impacts in Precambrian shields. Springer-Verlag, Berlin, pp. 117–171.
Naumov, M.V., 2005. Principal features of impact-generated hydrothermal circulation systems: Mineralogical and geochemical evidence. Geofluids 5, 165–184.
Newsom, H.E., 1980. Hydrothermal alteration of impact melt sheets with implications for Mars. Icarus 44, 207–216.
Newsom, H.E., Graup, G., Sewards, T., Keil, K., 1986. Fluidization and hydrothermal alteration of the suevite deposit in the Ries crater, West Germany, and implications for Mars. J. Geophys. Res. 91, 239–251.
Newsom, H.E., Brittelle, G.E., Hibbitts, C.A., Crossey, L.J., Kudo, A.M., 1996. Impact crater lakes on Mars. J. Geophys. Res. 101, 14951–14955.
Osinski, G.R., 2005a. Hydrothermal activity associated with the Ries impact event, Germany. Geofluids 5, 202–220.
Osinski, G.R., 2005b. Geological map, Haughton impact structure, Devon Island, Nunavut, Canada. Meteorit. Planet. Sci. 40 (Suppl.).
Osinski, G.R., Lee, P., 2005. Intra-crater sedimentary deposits at the Haughton impact structure, Devon Island, Canadian High Arctic. Meteorit. Planet. Sci. 40, 1887–1900.
Osinski, G.R., Spray, J.G., 2005. Tectonics of complex crater formation as revealed by the Haughton impact structure, Devon Island, Canadian High Arctic. Meteorit. Planet. Sci. 40, 1813–1834.
Osinski, G.R., Spray, J.G., Lee, P., 2001. Impact-induced hydrothermal activity within the Haughton impact structure, Arctic Canada; generation of a transient, warm, wet oasis. Meteorit. Planet. Sci. 36, 731–745.
Osinski, G.R., Grieve, R.a.F., Spray, J.G., 2004. The nature of the groundmass of surficial suevites from the Ries impact structure, Germany, and constraints on its origin. Meteorit. Planet. Sci. 39, 1655–1684.
Osinski, G.R., Lee, P., Parnell, J., Spray, J.G., Baron, M., 2005. A case study of impact-induced hydrothermal activity: The Haughton impact structure, Devon Island, Canadian High Arctic. Meteorit. Planet. Sci. 40, 1859–1878.
Osinski, G.R., Tornabene, L.L., Grieve, R.a.F., 2011. Impact ejecta emplacement on the terrestrial planets. Earth Planet. Sci. Lett. 310, 167–181.
Parnell, J., Lee, P., Cockell, C.S., Osinski, G.R., 2004. Microbial colonization in impact-generated hydrothermal sulphate deposits, Haughton impact structure, and implications for sulphates on Mars. Int. J. Astrobiol. 3, 247–256.
Parnell, J., Bowden, S., Osinski, G.R., Taylor, C.W., Lee, P., 2008. The transfer of organic signatures from bedrock to sediment. Chem. Geol. 247, 242–252.
Parnell, J. et al., 2010. Sulfur isotope signatures for rapid colonization of an impact crater by thermophilic microbes. Geology 38, 271–274.
Pirajno, F., 1992. Hydrothermal Mineral Deposits – Principles and Fundamental Concepts for the Exploration Geologist. Springer-Verlag, Berlin, Heidelberg.
Preston, L.J., Benedix, G.K., Genge, M.J., Sephton, M.A., 2008. A multidisciplinary study of silica sinter deposits with applications to silica identification and detection of fossil life on Mars. Icarus 198, 331–350.
Preston, L.J., Shuster, J., Fernández-Remolar, D., Banerjee, N.R., Osinski, G.R., Southam, G., 2011. The preservation and degradation of filamentous bacteria and biomolecules within iron oxide deposits at Rio Tinto, Spain. Geobiology 9, 233–249.
Rathbun, J.A., Squyres, S.W., 2002. Hydrothermal systems associated with martian impact craters. Icarus 157, 362–372.
Salger, M.V., 1977. Die tonminerale der forschungsbohrung Nördlingen 1973. Geol. Bavar. 75, 67–73.
Schelble, R.T., Westall, F., Allen, C.C., 2004. ~1.8 Ga iron-mineralized microbiota from the Gunflint Iron Formation, Ontario, Canada: Implications for Mars. Adv. Space Res. 33, 1268–1273.
Schopf, J.W., Kudryavtsev, A.B., Czaja, A.D., Tripathi, A.B., 2007. Evidence of Archean life: Stromatolites and microfossils. Precambrian Res. 158, 141–155.
Schulze-Makuch, D., Dohm, J.M., Fan, C., Fairen, A.G., Rodriguez, J.a.P., Baker, V.R., Fink, W., 2007. Exploration of hydrothermal targets on Mars. Icarus 308, 189–204.
Schwenzer, S.P., Kring, D.A., 2009. Impact-generated hydrothermal systems capable of forming phyllosilicates on Noachian Mars. Geology 37, 1091–1094.
Schwenzer, S.P. et al., 2012. Puncturing Mars: How impact craters interact with the martian cryosphere. Earth Planet. Sci. Lett. 335–336, 9–17.
Schwertmann, U., Murad, E., 1983. Effect of pH on the formation of goethite and hematite from ferrihydrite. Clays Clay Miner. 31, 277–284.
Strom, R.G., Malhotra, R., Ito, T., Yoshida, F., Kring, D.A., 2005. The origin of planetary impactors in the inner Solar System. Science, 1847–1850.
Tornabene, L.L., Osinski, G.R., Mcewan, A.S., 2009. Parautochthonous megabreccias and possible evidence of impact-induced hydrothermal alteration in Holden Crater, Mars. Lunar Planet. Sci. 40. 1766 pdf.
Wanger, G., Onstott, T.C., Southam, G., 2008. Stars of the terrestrial deep subsurface: A novel 'star-shaped' bacterial morphotype from a South African platinum mine. Geobiology 6, 325–330.
Zürcher, L., Kring, D.A., 2004. Hydrothermal alteration in the core of the Yaxcopoil-1 borehole, Chicxulub impact structure, Mexico. Meteorit. Planet. Sci. 39, 1199–1221.